DOI: 10.26599/FSHW.2026.9251125

Contents lists available at SciOpen

Food Science and Human Wellness

journal homepage: https://www.sciopen.com/journal/2097-0765

China Food Publishing Co.

Unraveling the Key Pathways through Cordycepin Prolongs Lifespan in *C. elegans* by Integrating Multi-omics Approaches

Shu Li[1], Hao Shi[2], Xin Yan[2], Yuqin Tong[1], Hui Yu[1], Hongmei Wang[1], Bo Deng[1], Chenglun Tang[4], Tao Shen[3], Hansheng Zhu[2], Yiping Chen[2], Yue Zhou[2], Changyi Huang[2], Hanjie Ying[3], Songtao Wang[1]*, Jian Zhao [2]*

[1] *Luzhou Pinchuang Technology Co., Ltd. (National Engineering Research Center of Solid-state Brewing), Luzhou, 646000, China*

[2] *Key Laboratory of Biological Resource and Ecological Environment of Chinese Education Ministry, College of Life Sciences, Sichuan University, Chengdu, 610064, China*

[3] *College of Biotechnology and Pharmaceutical Engineering, Nanjing Tech University, Nanjing, 211816, China*

[4] *Jiangsu Institute of Industrial Biotechnology, JITRI Co., Ltd., Nanjing, 210031, China*

ABSTRACT: Cordycepin, a food-derived bioactive nucleoside from *Cordyceps* exhibits anti-aging properties, yet its mechanisms in *Caenorhabditis elegans* remain unclear. We demonstrate that cordycepin (0.1–0.5 mg/mL) extended lifespan by 10-12% under both normal and heat-stress conditions while improving multiple healthspan parameters without reproductive tradeoffs. Integrative analysis combining network pharmacology, multi-omics profiling, and genetic validation identified the insulin/IGF-1 signaling (IIS) pathway as a central mediator. Network pharmacology and molecular docking implicated an IIS-associated upstream node, with IGF-1R/DAF-2 emerging as a computationally prioritized candidate, while functional assays showed that cordycepin promotes DAF-16 nuclear enrichment and requires DAF-16 to extend lifespan. Transcriptomic analysis identified 3,755 differentially expressed genes (DEGs) enriched in FOXO signaling, autophagy, and stress response pathways, with Weighted correlation network analysis identifying 15 hub genes linked to longevity traits. Metabolomics detected 267 differentially expressed metabolites, highlighting enhanced glutathione-mediated antioxidant defense and remodeling of lipid metabolism centered on glycerol-3-phosphate, a membrane phospholipid precursor. Microbiome analysis showed selective enrichment of *Bacillus* spp. with positive lifespan correlation. Multi-omics integration revealed that cordycepin-mediated DAF-16 activation coordinates transcriptional reprogramming, metabolic homeostasis, and potential microbiome modulation through the conserved IIS/FOXO axis. This study supports cordycepin as a promising pro-longevity bioactive that functionally converges on evolutionarily conserved longevity pathways, while direct upstream target engagement remains to be established.

Keywords: Cordycepin; *C. elegans*; Lifespan extension; Multi-omics; Network pharmacology.

1. Introduction

In recent years, as the global population ages, research focused on extending lifespan and improving health has gained increasing importance [1, 2]. Although dietary interventions such as caloric restriction and

***Corresponding author**
SongTao Wang: wangst@lzlj.com; Jian Zhao: zj804@163.com

Received 26 May 2025
Received in revised from 21 July 2025
Accepted 20 March 2026

fasting regimens demonstrate robust pro-longevity effects across evolutionarily diverse species [3], their practical challenges have motivated the search for pharmacological alternatives—compounds that mimic dietary restriction's molecular benefits without requiring lifestyle modifications. Natural bioactive small molecules derived from food sources, including teaseed oil, curcumin, and luteolin, extend lifespan through modulation of conserved longevity pathways [4-6], offering superior safety profiles and economic accessibility compared to synthetic interventions [7, 8]. Among these natural compounds, nucleoside-related metabolites represent a particularly intriguing class. Dietary supplementation with pyrimidine pathway intermediates extends *C. elegans* lifespan by modulating reproductive signaling through DAF-12, NHR-49, and DAF-16/FOXO [9]. Yet the organism-level longevity mechanisms of individual nucleoside constituents remain incompletely characterized [10]. Cordycepin (3′-deoxyadenosine), the characteristic nucleoside analog from *Cordyceps sinensis* [11, 12], exemplifies this knowledge gap. While cordycepin influences gene expression, nucleic acid synthesis, and signal transduction [13-17], exhibiting diverse activities including immune modulation [18-24] and anti-aging properties in mammalian models (enhanced antioxidant enzymes, reduced lipid peroxidation) [25-27], its mechanisms in *C. elegans*—a premier genetic model for aging research [28-30]—remain uncharacterized. This contrasts with the mechanistic elucidation of other natural compounds in *C. elegans*: rebaudioside A enhances oxidative stress resistance [31], tomatidine induces mitophagy via SKN-1/Nrf2 [32], patchouli oil activates JNK-1/DAF-16 [33], lentinan coordinates DAF-16 and SKN-1 [34], and teaseed oil elicits metabolic reprogramming [6]. These studies reveal that natural products often converge on conserved longevity networks—particularly insulin/IGF-1 signaling (IIS) [35, 36], dietary restriction mimetics [37, 38], and stress-responsive pathways [39-41]—while exhibiting compound-specific upstream entry points.

The mechanistic complexity of nucleoside analogs, combined with the highly interconnected nature of *C. elegans* longevity regulation (encompassing insulin/IGF-1 signaling, dietary restriction responses [37, 38], reproductive signaling [42], mitochondrial dynamics [43], and stress-responsive pathways [41]), necessitates a comprehensive systems-level investigation. Recent advances in integrated multi-omics methodologies—transcriptomics, metabolomics, and microbiome profiling—have proven indispensable for elucidating pleiotropic mechanisms of bioactive compounds by enabling simultaneous interrogation of gene expression, metabolite flux, and microbial community structure [31-34]. Crucially, the synergistic integration of multi-omics data, network pharmacology, and functional genetics offers a robust framework to deconvolute the complex anti-aging effects and their underlying molecular mechanisms.

To comprehensively elucidate the molecular mechanisms underlying cordycepin-mediated lifespan extension in *C. elegans*, this study integrates phenotypic characterization, multi-omics profiling (microbiome, transcriptomics, metabolomics), network pharmacology, and functional genetics. We pursued three specific aims: (1) to prioritize candidate upstream nodes potentially involved in cordycepin-mediated longevity using network pharmacology and molecular docking, and to test pathway-level involvement using genetic epistasis in *daf-2* and *daf-16* mutants, DAF-16::GFP reporter-based localization assays, and targeted gene expression profiling; (2) to characterize cordycepin-induced perturbations across transcriptional (differentially expressed

genes and pathway enrichment), metabolic (differentially expressed metabolites and metabolic network remodeling), and microbiome (community structure and host-microbe interactions) layers; and (3) to integrate multi-omics datasets through weighted gene co-expression network analysis (WGCNA), gene-metabolite correlation, and microbiome-metabolite association modeling (MIMOSA2) to delineate the molecular interplay underpinning cordycepin's pro-longevity effects. The findings advance fundamental understanding of how cordycepin analogs modulate longevity through conserved regulatory networks.

2. Materials and Methods

2.1. Chemicals

Cordycepin was prepared from *Cordyceps sinensis* using a membrane-separation procedure. Briefly, the crude extract was subjected to high-pressure homogenization at a 1:10 (w/v) solid–liquid ratio, followed by ultrafiltration to remove macromolecular impurities. The filtrate was then concentrated by nanofiltration to a final cordycepin concentration of 50–60 g/L, and cordycepin was obtained by low-temperature crystallization at 0–4 °C for 10 h. The purity of cordycepin was compared with LC–MS/MS analysis against a commercial cordycepin reference standard, which supported high sample purity (estimated at 99.2%). The mobile phase consisted of 0.01 mol/L KH_2PO_4: methanol (75:25, v/v) at a flow rate of 1.0 mL/min, with an injection volume of 20 μL.

2.2 Strains and Culture Conditions

Wild-type *C. elegans* N2 (obtained from the Key Laboratory of Biological Resource and Ecological Environment of Chinese Education Ministry, College of Life Sciences, Sichuan University) were maintained at 20 °C on solid nematode growth medium (NGM) plates seeded with *E. coli* OP50. The mutant strains used in this study, including TJ356 (DAF-16::GFP), *daf-2* (e1370), and *daf-16* (mu86), were obtained from the Caenorhabditis Genetics Center (CGC) and maintained under the same standard conditions. To synchronize the population, gravid adults were treated with 1% (v/v) sodium hypochlorite and 0.25 M NaOH for 5–7 min to isolate eggs. The eggs were incubated in M9 buffer overnight at 20°C to hatch into L1 larvae, which were then transferred to fresh NGM plates and cultured until L4 larvae [44, 45]. NGM was prepared using 3 g/L NaCl, 17 g/L agar, and 2.5 g/L peptone, and supplemented after autoclaving with cholesterol, $CaCl_2$, $MgSO_4$, and potassium phosphate buffer (pH 6.0). Media were autoclaved at 121 °C for 15 min prior to plate pouring.

2.3 Heat Stress Assay

The anti-heat-stress assays were performed using synchronized L4-stage *C. elegans* ($n \geq 30$ per group; $\geq$ 3 independent replicates) cultured on NGM plates under standard conditions with cordycepin (0–100 mg/mL, dissolved in 0.1% DMSO) or a 0.1% DMSO control. Nematodes were exposed to 35°C in an environmental chamber, with survival quantified hourly until complete mortality [46]. DMSO was used only in this acute heat-stress screening assay; for lifespan and multi-omics experiments, sterile water was used as vehicle control.

2.4 Nematode Lifespan Assays

Lifespan assays were performed with a minimum of 30 animals per group, and each experiment was independently repeated at least three times [47, 48]. L4-stage nematodes were initially transferred to NGM plates supplemented with 40 μM 5'-fluorodeoxyuridine (FUDR) for 2 days to prevent reproduction [49]. Post-treatment nematodes were maintained on FUDR-free NGM plates supplemented with cordycepin (prepared in sterile water; no DMSO) or sterile water as the vehicle control at the specified concentration, with adult day 1 designated as the first day of post-developmental maturity. To mitigate mating-induced heterogeneity and nutritional depletion, nematodes were transferred daily during the initial 5-day reproductive period and biennially thereafter. Cultures were maintained at 20°C, with survival assessed daily until group extinction. Epistasis lifespan assays in *daf-2* (e1370) and *daf-16* (mu86) mutants were performed under the same conditions.

2.5 Body Length, Reproduction, Pharyngeal Pumping, and Locomotion Assays

Growth measurements were conducted in parallel with the longevity assay on days 4, 7, 10, and 13 of survival. For each time point, at least 30 nematodes per group were randomly selected from each group and analyzed for body length using ImageJ software (National Institutes of Health, USA) [50].

Reproduction assays involved randomly selecting L4-stage nematodes (pre-treated as described in the longevity experiment), which were transferred to fresh NGM plates (with 3 biological replicates per group) every 24 hours throughout the reproductive period. Eggs were counted immediately after adults were transferred to a new plate to determine both daily and total egg production for each group of 10 nematodes.

Pharyngeal pumping was assessed in conjunction with the longevity assay by recording the number of pharyngeal contractions over 15 seconds, at 2-day intervals, starting from day 1 of the longevity experiment. At least 5 nematodes were randomly selected from each group (3 biological replicates per group) for this analysis [51].

Locomotion assays were also aligned with the longevity assay. Beginning on day 1 of the longevity recording, at least 10 nematodes per group (3 biological replicates per group) were selected and dropwise added a single drop of M9 buffer. The number of body swings (back-and-forth movements) was counted under a microscope over 20 seconds. This measurement was recorded at 2-day intervals throughout the experiment [52].

2.6 DNA Extraction and Amplicon Sequencing Analysis

DNA was extracted from approximately 10,000 nematodes per sample. Samples were divided into control group day 0 (C00), control group day 7 (C07), and cordycepin treatment day 7 (CC7) with three biological replicates, and DNA was extracted using the FastDNA® Spin Kit for Soil (MP Biomedicals, USA) following the manufacturer's instructions. The extracted DNA was then subjected to amplicon sequencing. Specifically, the V3-V4 region of the 16S rRNA gene (Forward primer (341F): 5'-CCTACGGGNGGCWGCAG-3', reverse primer (805R): 5'-GACTACHVGGGTATCTAATCC-3') was amplified. The amplicons were sequenced using 250 bp paired-end sequencing on a MiSeq benchtop sequencer. Raw sequence data were quality filtered and merged, removing barcodes using FLASH [53]. Clean

reads were obtained by eliminating chimeras and low-quality sequences using USEARCH v.10.0.240. Data processing and analysis were performed using QIIME v.1.9.1 [54] and R v.2.3-5. Operational taxonomic units (OTUs) were clustered at a 97% similarity threshold using UPARSE version 7.1 [55]. Representative **bacterial** OTU sequences were annotated and analyzed against 16S rRNA gene databases using the RDP Classifier version 2.2 [56]. Group labels (similarly hereinafter): "C" denotes vehicle control and "CC" denotes cordycepin-treated worms (0.1 mg/mL, unless stated otherwise); the number indicates adult day at sampling. Thus, C00 = control at adult day 0, C07 = control at adult day 7, and CC7 = cordycepin at adult day 7.

2.7 RNA Extraction and Transcriptome Analysis

Total RNA isolation from synchronized groups (three biological replicates per group, aligned with microbiome experimental design) was performed via TRIzol® reagent (Invitrogen, USA), followed by genomic DNA elimination using DNase I (Takara, Japan). RNA integrity underwent dual verification: spectrophotometric quantification (NanoDrop2000, USA; OD260/280 1.8–2.2, OD260/230 >2.0) and electrophoretic resolution (1.5% agarose gel, 28S:18S ≥1.0), with RNA Integrity Numbers (RIN ≥6.5) confirmed via 2100 Bioanalyzer (Agilent, USA). Library construction proceeded exclusively for samples meeting inclusion thresholds: total RNA mass ≥1 μg, RIN ≥6.5 [57]. Polyadenylated mRNA enrichment preceded cDNA synthesis (reverse transcription), with 300 bp fragments isolated by 2% low-melt agarose size fractionation. Paired-end sequencing (Illumina NovaSeq6000) generated raw reads subjected to quality trimming, read mapping, and transcript quantification, followed by differential expression analysis (DESeq2; significance: |log2FC| >0, $P < 0.05$). KEGG pathway enrichment analysis elucidated functional profiles of differentially expressed genes (DEGs) [58].

2.8 Untargeted LC-MS/MS Analysis

For comparative metabolomic analysis, synchronized groups of *C. elegans* (n ≈ 10,000 per treatment; six biological replicates per group, aligned with microbiome experimental design) underwent homogenization in 400 μL 80% methanol (v/v) supplemented with 0.02 mg/mL L-2-chloro-phenylalanine (internal standard) via lyophilization at -10°C (6 min). Following cryogenic sonication (40 kHz, 30 min, 5°C) and subsequent refrigeration (-20°C, 30 min), cellular debris was pelleted by centrifugation (13,000 rpm, 15 min, 4°C), with clarified supernatants retained for LC-MS analysis. Metabolite separation was achieved using a UHPLC-Q Exactive HF-X system (Thermo Scientific, China) equipped with an ACQUITY UPLC HSS T3 column (100 × 2.1 mm, 1.8 μm; Waters, Milford, USA), with mobile phases comprising 5% aqueous acetonitrile and 47.5% acetonitrile/47.5% isopropanol. Electrospray ionization (ESI) was performed at 40°C, with dual-polarity data acquisition (positive/negative modes) at 60,000 resolution across m/z 70–1050 [59]. Capillary and source temperatures were maintained at 325°C. Multivariate statistical analyses (PCA, PLS-DA) derived Variable Importance in Projection (VIP) scores, complemented by univariate t-tests ($P < 0.05$ threshold). Differentially expressed metabolites (DEMs; VIP > 1, $P < 0.05$) underwent functional annotation via KEGG (http://www.genome.jp/kegg/) and HMDB (http://www.hmdb.ca/) databases [60].

2.9 RT-qPCR and qPCR Analysis

Following a 7-day cordycepin exposure regimen, *C. elegans* specimens were harvested and subjected to triple-wash cycles with M9 buffer to ensure bacterial clearance. Genomic DNA isolation was performed using the TaKaRa MiniBEST Universal Genomic DNA Extraction Kit (Takara Bio, Japan). Quantitative PCR (qPCR) was performed with PowerUp™ SYBR Green Master Mix (Tsingke Biotechnology, Beijing, China). Relative *telG* expression levels were normalized to the housekeeping gene *actin-1* (*act-1*) and calculated via the $2^{-\Delta\Delta C_T}$ method. For telomere length quantification, references previously described methods [61]. All experiments incorporated three independent biological replicates, each analyzed in triplicate. Statistical significance was assessed via unpaired two-tailed Student's *t*-tests, with data presented as mean ± standard deviation (SD). In addition, targeted RT–qPCR was performed (using the same SYBR Green workflow) to quantify the expression of canonical DAF-16 target genes (*sod-3*, *ctl-1*, *hsp-16.1*, *lys-7*, *gst-4*) [62] and AMPK components (*aak-2* and *aakg-1*; primers in Table S1) [63] in worms treated with cordycepin (0.1 mg/mL) and control, and results were expressed as fold change relative to control.

2.10 Network pharmacology and molecular docking

Network pharmacology was employed to prioritize candidate longevity-associated targets potentially related to cordycepin action. The target proteins of cordycepin were predicted using PharmMapper (https://lilabecust.cn/pharmmapper) and TCMSP (https://old.tcmsp-e.com/tcmsp.php). Genes associated with human aging were obtained from multiple databases, including HAGR (https://www.genomics.senescence.info), GeneCards (https://www.genecards.org/), and TTD (https://db.idrblab.net/ttd/). Venny 2.1.0 was used to identify common targets, and protein-protein interaction (PPI) networks were constructed using the STRING database (https://string-db.org). Network topology parameters were calculated using the Cytoscape Network Analyzer, enabling the identification of potential anti-aging targets of cordycepin. Because this analysis was based on human aging-related databases and docking to the human IGF-1R structure, it should be interpreted as cross-species candidate prioritization rather than direct target identification in *C. elegans*.

2.11 DAF-16::GFP subcellular localization assay

TJ356 (DAF-16::GFP) worms were synchronized and transferred to NGM agar plates supplemented with cordycepin (0.1 mg/mL) or a blank control at the L1 stage. DAF-16::GFP localization was examined at adult Day 2 and adult Day 7, and images were captured using a Zeiss Axioskop 2 plus fluorescence microscope (Carl Zeiss, Jena, Germany) equipped with a digital camera. DAF-16::GFP subcellular distribution was scored as cytosolic, intermediate, or nuclear based on nuclear enrichment, and the percentage of animals in each category was quantified (ImageJ, NIH). Three plates, each containing 30 animals, were analyzed per assay, and all experiments were performed independently three times.

2.12 Data Analysis

All experiments were conducted with a minimum of three independent biological replicates. Data are presented as mean ± SEM in all figures. Survival curves were analyzed by Kaplan–Meier estimation and

compared using the log-rank (Mantel–Cox) test. For comparisons between two groups, a Student's t-test was applied, while one-way ANOVA was used for comparisons involving three or more groups. A p-value of < 0.05 was considered statistically significant. Statistical analysis and graphing were performed using GraphPad Prism 9.0.

3. Results

3.1 Cordycepin Exhibits Pro-Longevity Effects in C. elegans

Initially, a biphasic dose-response relationship was observed in *C. elegans* subjected to 35°C thermal challenge following cordycepin pretreatment (0.05–100 mg/mL), with survival kinetics revealing concentration-dependent modulation of thermotolerant lifespan (Fig. 1A). Sub-pharmacodynamic doses (≤10 mg/mL) induced significant median survival extension ($P < 0.05$), evidenced by rightward survival curve displacement post-11 h thermal exposure, peaking at 0.1 mg/mL. Conversely, supraphysiological concentrations (≥50 mg/mL) exhibited pronounced longevity inhibition relative to the 0.1% DMSO vehicle control in the acute heat-stress dose-range screening assay, establishing 0.1 mg/mL as the therapeutic ceiling for subsequent experimental standardization.

Non-monotonic enhancement of *C. elegans* longevity under normothermic conditions (20°C) was observed across cordycepin doses (0.1–5 mg/mL), with maximal geroprotective efficacy at 0.1 mg/mL (23.64 d mean lifespan; +12.43%, $P < 0.001$ vs control) and 0.5 mg/mL (23.14 d; +10.04%, $P < 0.01$) (Fig. 1B-F; Table 1). All sub-10 mg/mL interventions elevated longevity indices (mean/median/maximum survival), establishing 10 mg/mL as a pharmacological ceiling for lifespan benefits. Telomere length analysis via qPCR revealed non-significant elongation trends in cordycepin-treated specimens versus controls ($P >0.05$; Fig. S1).

Table 1. Effect of cordycepin on median survival time and mean lifespan of nematodes (Mean ± SD, n = 90)

Groups (mg/mL)	Life expectancy (d)	Life expectancy up (%)	Median survival time (d)	Maximum survival time (d)
Control	21.03±3.07	-	21	25
0.1	23.64±2.81***	12.43	25	29
0.5	23.14±4.26**	10.04	25	29
1	22.11±3.21	5.15	25	29
5	22.31±5.27	6.08	23	33
10	13.12±4.75****	-37.61	15	27

Cordycepin significantly influences both the median survival time and the mean lifespan of nematodes. Statistical significance compared to the blank control group is indicated as follows: **$P < 0.01$, ***$P < 0.001$, ****$P < 0.0001$.

3.2 Cordycepin Promoted Key Phenotypic Traits Including Body Length and Locomotion in C. elegans, While Maintaining Baseline Reproductive Capacity

Contrary to established evolutionary trade-offs positing longevity-fecundity antagonism [64-67], subtoxic cordycepin concentrations (0.1–0.5 mg/mL) had no significant impact on nematode fecundity (Fig. 1G, H). Biphasic somatic modulation was observed in *C. elegans* under cordycepin exposure (0.1–10 mg/mL), with maximal morphometric augmentation at 0.5 mg/mL (1854.45 μm day 7; 1937.85 μm day 13, $P < 0.05$ vs. untreated groups), while subtherapeutic (0.1/1 mg/mL) and suprapharmacological (≥5 mg/mL) doses elicited

non-significant expansion or attenuated body length, respectively (Fig. 1I-K; Fig. S2; Table S2). Mid-exposure intervals (days 7–13) revealed dose-dependent divergence, as 0.5 mg/mL induced sustained length growth, whereas higher concentrations (≥5 mg/mL) suppressed body size despite null statistical significance across measurement periods.

Pharyngeal pumping frequency exhibited dose-dependent temporal decoupling: 0.1 mg/mL induced significant elevation during days 10–13 ($P < 0.05$ vs. controls), while 0.5 mg/mL enhanced pumping days 7–10 ($P < 0.05$), paralleled by sustained motility augmentation through day 16 ($P < 0.01$) (Fig. 1L, M). However, suprapharmacological doses (≥5 mg/mL) suppressed pharyngeal and mobility activity within discrete temporal windows. These findings suggest that lower concentrations may enhance both pharyngeal activity and locomotor function without compromising reproductive success.

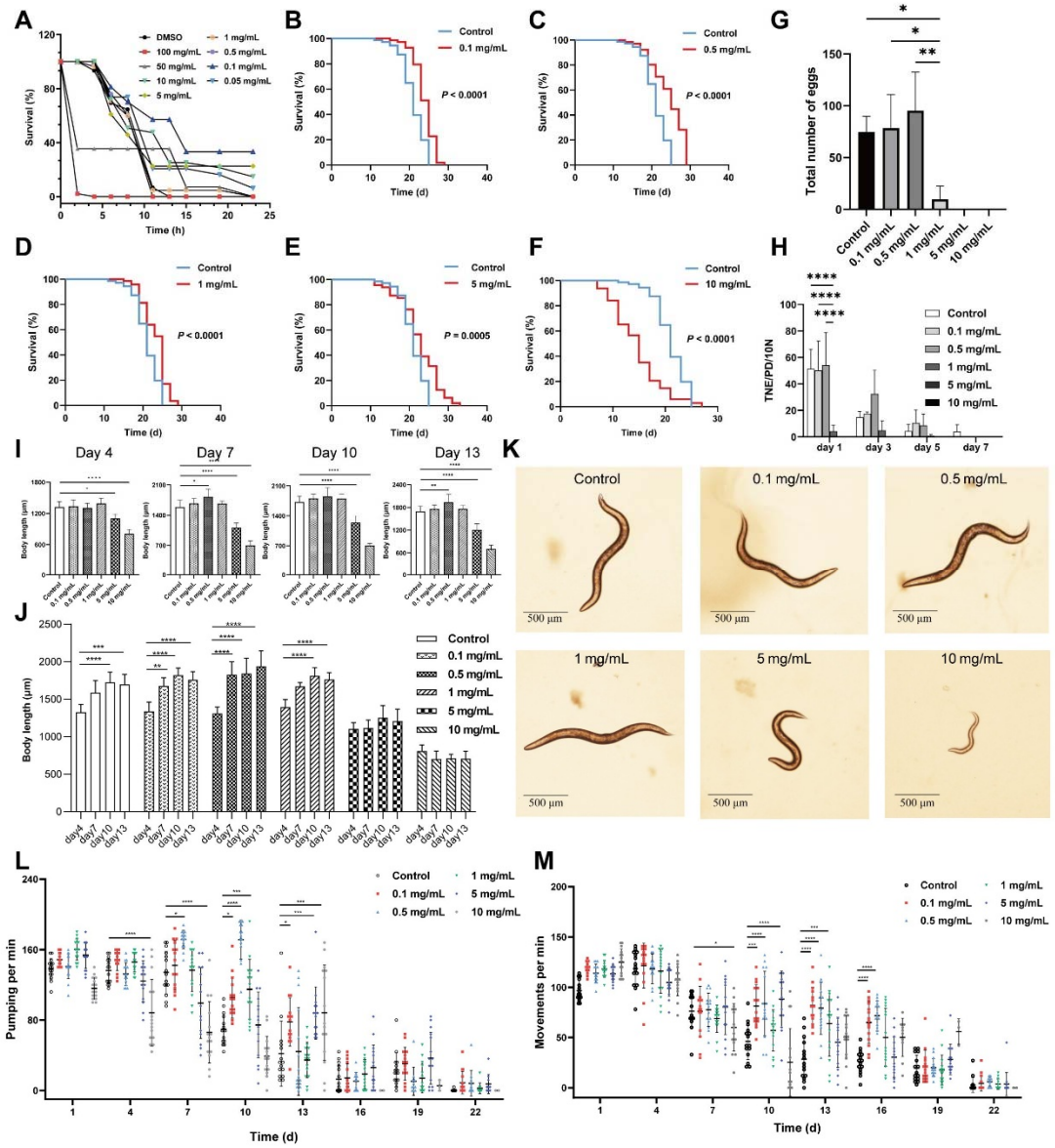

Fig. 1 Cordycepin's concentration-dependent modulation of *Caenorhabditis elegans* physiology under thermal and basal conditions.

(A–F) Thermal-stress assays and lifespan analyses (***$P < 0.001$, **$P < 0.01$; *$P < 0.05$; log-rank test). (G, H) Reproductive output and cumulative egg counts. (****$P < 0.0001$, ***$P < 0.001$, **$P < 0.01$; *$P < 0.05$, Tukey's multiple comparisons test) (I–K) Body length comparisons (L, M) Pharyngeal pumping frequency and locomotor activity. Data expressed as mean ± SEM. TNE/PD/10N, Total number of eggs per day per 10 nematodes; SEM, standard error of the mean; ANOVA, analysis of variance; DMSO, dimethyl sulfoxide.

3.3 Selective Bacillus enrichment in cordycepin-treated C. elegans

Dose-response optimization identified 0.1 mg/mL cordycepin as the concentration achieving maximal lifespan extension and healthspan enhancement in *C. elegans*. This threshold was prioritized for multi-omics interrogation to isolate geroprotective mechanisms from stress-related confounding effects. Comparative 16S rRNA sequencing of Cordycepin-treated and control nematode groups, analyzed on days 0 and 7 post-M9 buffer rinsing, demonstrated stratified microbiome dynamics. Venn diagrams illustrated average operational taxonomic unit (OTU) counts and intergroup overlap (Fig. 2A), with *E. coli* dominating (>91% relative abundance; Table S3). α-Diversity quantification revealed community complexity: C00 group exhibited maximal diversity (Shannon index: 1.514 ± 0.086), CC7 group intermediate richness (0.130±0.010), and C07 group marked depletion (0.093±0.012; Table S4). Subsequent analyses excluded *E. coli* to elucidate treatment-induced shifts in taxa (Fig. 2B–G). Multivariate analyses (PCoA, ANOSIM) confirmed significant Cordycepin-induced divergence in microbial β-diversity relative to controls (Fig. 2B, C). At the phylum level, Actinobacteriota abundance increased with growth time, while Chloroflexi abundance decreased. Notably, Firmicutes abundance rose more prominently in the CC7 group compared to the control, with all other phyla showing significant decreases (Fig. 2D, E). At the genus level, uncultured 966-1 and *Candidatus_Competibacter* abundances declined over time, while *Enterobacter*, *Ralstonia*, and *Sphingomonas* abundances increased. *Bacillus* abundance was significantly higher in the CC7 group compared to the control (Fig. 2F, G). Linear discriminant analysis (LEfSe) identified *Bacillus* as a signature microorganism of the treated group, with its abundance increasing distinctly (Fig. 2I). Co-occurrence network analysis corroborated genus-level microbiome and nematode phenotype linkages (Fig. S3A). Correlation analyses revealed *Candidatus* and *Alistipes* abundances were inversely associated with longevity and body-length metrics, while *Bacillus* exhibited a positive lifespan correlation (Fig. S3B). Subsequent two-factor network analysis confirmed *Bacillus* as the sole genus demonstrating a significant pro-longevity association (Fig. S3C). These findings implicate cordycepin supplementation in structural and functional microbiome modulations underlying observed phenotypic outcomes.

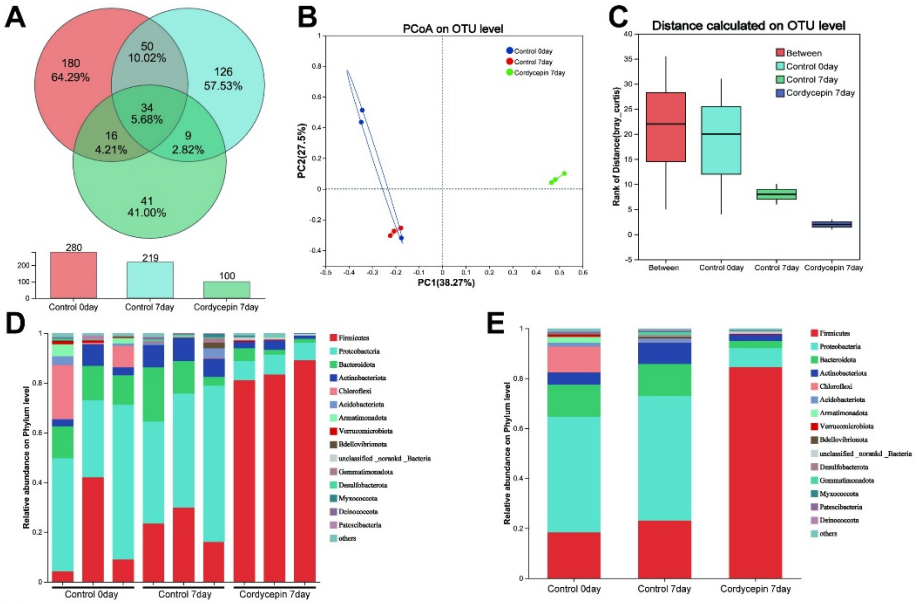

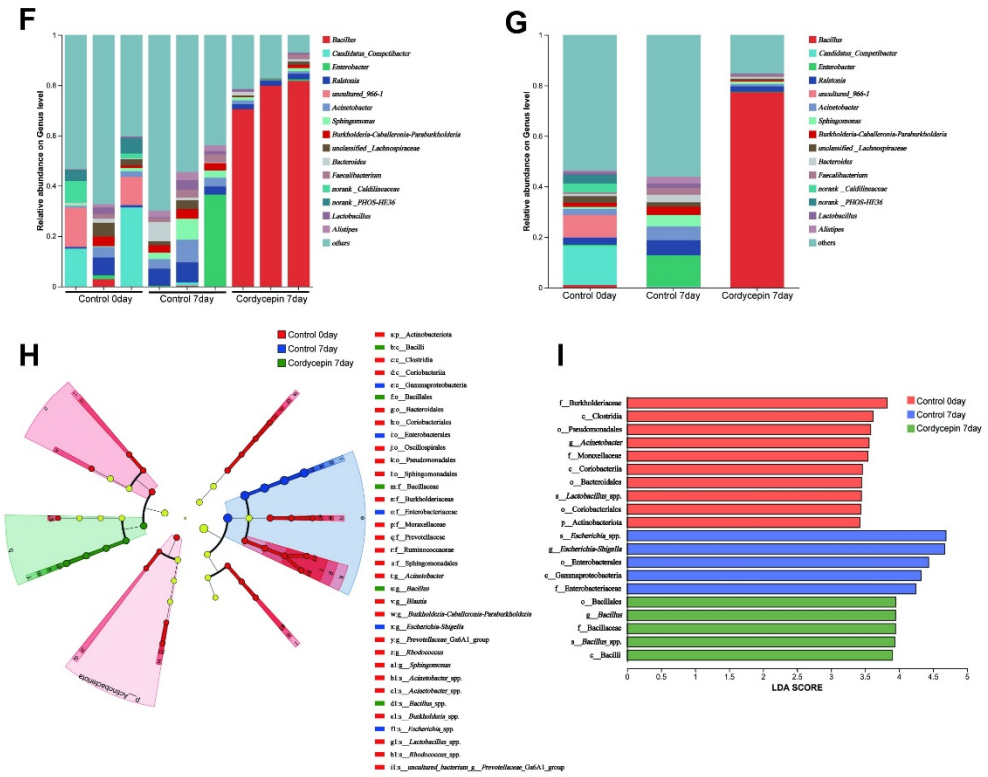

Fig. 2 Cordycepin modulates the microbiota of *Caenorhabditis elegans*.
(A) Venn diagram of shared OTUs among treatment groups over time. (B) PCoA clustering microbial communities. (C) ANOSIM of inter-group compositional differences. (D) Phylum-level taxonomic composition (bar plots). (E) Phylum distribution histogram across groups. (F) Genus-level community structure variations. (G) Nematode-associated genera (columnar analysis). (H-I) LEfSe discriminant taxa with contribution ranking. OTUs, Operational Taxonomic Units; PCoA, Principal Coordinates Analysis; ANOSIM, Analysis of Similarities; LEfSe, Linear discriminant analysis Effect Size; LDA, Linear Discriminant Analysis.

3.4 Cordycepin remodels metabolic homeostasis in C. elegans

3.4.1 Cordycepin contributes to a richer metabolite composition of C. elegans

Metabolomic perturbations in *C. elegans* exposed to 0.1 mg/mL Cordycepin were investigated via non-targeted LC-MS, revealing intervention-specific metabolic restructuring. Hierarchical clustering of normalized metabolite profiles (Fig. S4A) preceded multivariate analyses (PCA, PLS-DA), which delineated pronounced segregation between untreated and Cordycepin-treated groups (Fig. S4B, C), indicative of substantial metabolic reprogramming. Global profiling identified 691 metabolites, categorized hierarchically (Fig. S4D): lipids/lipid-like molecules (41.33%), organic acids/derivatives (19.70%), organic oxygen compounds (10.71%), organoheterocyclics (9.64%), nucleosides/nucleotides/analogs (6.00%), benzenoids (5.14%), organic nitrogen compounds (3.21%), phenylpropanoids/polyketides (2.78%), others (1.50%).

Stringent thresholds (VIP >1, |FC| >2.0, $P < 0.05$) resolved 225 differentially expressed metabolites (DEMs) in the C07 vs C00 group (184↑/41↓), 225 (170↑/55↓) in the CC7 vs C00 group, and 267 (97↑/170↓) in the CC7 vs C07 group (Fig. S4E–H). The CC7 vs C07 contrast exhibited maximal DEM abundance, suggesting Cordycepin-driven metabolic homeostasis modulation—a putative longevity correlate. Lipid-centric classes dominated DEM profiles, with top DEM expression trends and VIP scores detailed in supplementary visualizations (Fig. S5, S6).

3.4.2 FOXO Pathway Links Cordycepin's Metabolic Reprogramming and Antioxidant Effects

Sample clustering analysis demonstrated branch-specific segregation of differentially expressed metabolites (DEMs) across treatment conditions (Fig. 3A; S6A, C). While a phospholipid, lipid, and purine-related metabolite subset displayed selective upregulation, most phospholipids, lipids, alkaloids, nucleotides, and choline derivatives were broadly downregulated in CC7 vs C07 (Fig. 3A). KEGG enrichment analysis implicated purine/glycerophospholipid metabolism, ABC transporters, autophagy, and cofactor biosynthesis as central pathways (Fig. 3B). Comparative metabolomics of C07 vs C00 and CC7 vs C00 groups (Fig. S7B, D) revealed divergent enrichment profiles: C07 vs C00 showed prominence in purine/glycerophospholipid metabolism, tryptophan metabolism, GPI-anchor biosynthesis, and cofactors, whereas CC7 vs C00 exhibited ABC transporters, glutathione metabolism, and cofactor biosynthesis. Strikingly, ABC transporters and FOXO signaling emerged as uniquely differential pathways between groups, indicating cordycepin-driven FOXO pathway modulation and ABC transporter activity shifts. These data nominate ABC transporters as a central metabolic target, with therapeutic effects mediated via FOXO signaling and transmembrane transport regulation.

Recurrently significant metabolites within enriched pathways (Fig. 3C) displayed profound shifts under cordycepin treatment, including significantly elevated acetylcholine, glycerol 3-phosphate (a glycerophospholipid precursor), and glutathione, alongside suppressed adenosine monophosphate and guanosine. In line with this FOXO-dependent antioxidant program, cordycepin triggered a glutathione-centered response (Table S5). In addition to the increase in GSH levels, we observed a concomitant upregulation of the glutathione S-transferase omega gene *gsto-1* and higher mean expression of GSH biosynthetic and recycling enzymes such as *gcs-1*, *gss-1*, and *gsr-1*, as well as γ-glutamyl cycle components *C53D5.5* and *T03D8.6*, under cordycepin treatment. Furthermore, several GSH-dependent peroxidases (*gpx-1*, *gpx-5*, *gpx-6*, and *gpx-7*) were induced, whereas *gpx-2* showed reduced expression, suggesting isoform-specific tuning of GSH-linked redox defenses. Thus, cordycepin appears to be associated with a glutathione-centered antioxidant remodeling pattern alongside FOXO activation, consistent with enhanced stress resilience, although the current data do not determine whether this change is causally upstream of lifespan extension. Collectively, these results delineate a cordycepin-induced metabolomic reprogramming axis in *C. elegans*, mechanistically coupling metabolic state realignment, particularly in purine homeostasis, redox balance, and lipid signaling to lifespan extension. The findings underscore metabolic plasticity as a critical mediator of cordycepin’s geroprotective outcomes.

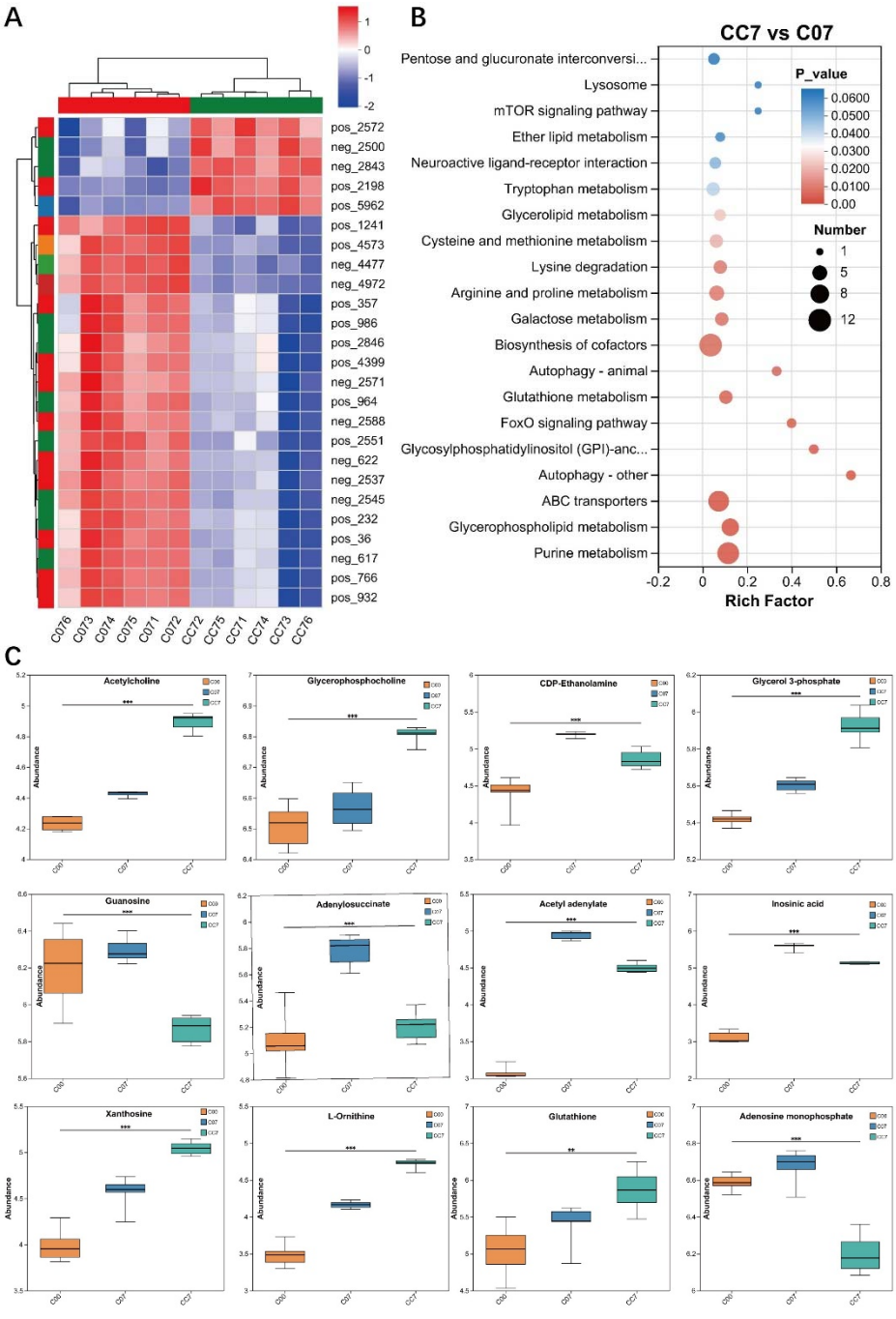

Fig. 3 Expression Profiling of DEMs and KEGG Pathway Enrichment Analysis

(A) Heatmap of differentially expressed metabolites (DEMs) in CC7 vs C07 groups. (B) Bubble plot of enriched KEGG pathways in CC7 vs C07. (C) Multi-group analysis of key metabolites in enriched pathways. DEMs, differentially expressed metabolites; KEGG, Kyoto Encyclopedia of Genes and Genomes; C00, control group day 0; C07, control group day 7; CC7, cordycepin treatment day 7; ANOVA, analysis of variance

3.5 Transcriptome-wide Analysis of Cordycepin Regulatory Mechanisms

High-throughput sequencing produced 64.1 Gb of high-fidelity data (Q20 >97.2%, Q30 >92.4%; GC content 46.9–48.8%), validating robust sequencing quality (Table S6). De novo transcriptome assembly generated 72,064 transcripts (61,452 non-redundant unigenes), with PCA demonstrating clear group segregation along primary variance axes (PC1 × PC2: 27.98% ×15.96%; Fig. 4B). Functional annotation

across six databases (GO, KEGG, EggNOG, NR, Pfam, SwissProt) systematically characterized molecular profiles (Table S7).

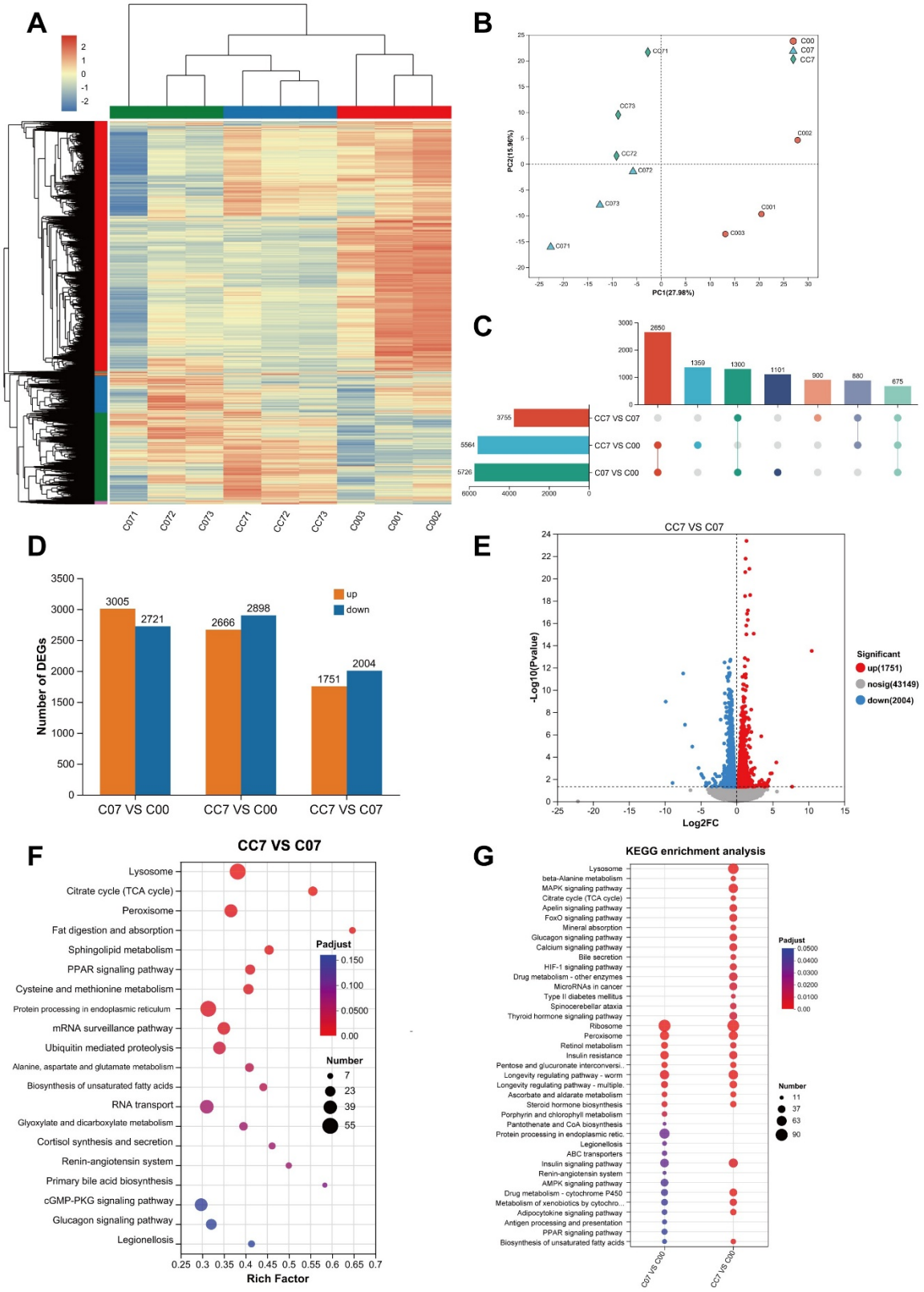

Fig. 4 Quality Control of Transcriptomic Data and Differentially Expressed Genes (DEGs) (A) Heatmap of differentially expressed genes (DEGs). (B) PCA shows sample variation. (C) Upset plot of overlapping relationships among groups. (D) Classification and proportional distribution of differentially expressed metabolites (DEMs). Volcano plots of DEMs in CC7 vs C07. (F) Enriched pathways in CC7 vs C07. (G) Comparative analysis of conserved/divergent pathways (CC7 vs C00 and C07 vs C00). DEGs, differentially expressed genes; PCA, Principal Component Analysis; KEGG, Kyoto Encyclopedia of Genes and Genomes; FC, fold change; C00, control group day 0; C07, control group day 7; CC7, cordycepin treatment day 7.

Differential expression analysis ($P < 0.05$, |log2FC| >0) identified distinct transcriptional dynamics, including a core conserved transcriptional program of 1,555 genes shared across cordycepin treatments (Fig. 4C), nominating central regulatory targets. Group-wise comparisons revealed 5,726 DEGs (C07 vs C00: 3,005↑, 2,721↓), 5,564 DEGs (CC7 vs C00: 2,666↑, 2,898↓), and 3,755 DEGs (CC7 vs C07: 1,751↑, 2,004↓) (Fig. 4D, E; Fig. S8A, B). The top 15 upregulated and downregulated DEGs (Table S8) and heatmap visualization (Fig. 4A) confirmed pronounced divergence in expression profiles among comparison groups.

3.5.1 Cordycepin reprograms multiple pathways in C. elegans to mediate longevity

KEGG pathway analysis identified ribosome, peroxisome, retinol metabolism, and insulin resistance as key pathways modulated during normal aging in *C. elegans*. (Fig. S8). Comparative analysis of the CC7 vs C00 groups further highlighted ribosome, lysosome, peroxisome, longevity regulating pathways, and steroid hormone biosynthesis as central metabolic hubs (Fig. S8D). Strikingly, the CC7 vs C07 comparison revealed peroxisome, lipid digestion, sphingolipid metabolism, and PPAR signaling as principal enriched pathways (Fig. 4F). Enrichment and comparative analysis profiling across CC7 vs C00 and C07 vs C00 groups demonstrated that cordycepin treatment induces marked shifts in gene expression, with pronounced enrichment in lysosome, MAPK signaling, FoxO signaling, HIF-1 signaling, and glucagon signaling pathway (Fig. 4G). KEGG pathway interrogation demonstrated that cordycepin administration primarily modulates lipid homeostasis, membrane architecture, and lysosomal processing, with concurrent pronounced enrichment of metabolic cascades mechanistically linked to longevity potentiation. These observations demonstrate functional convergence with complementary metabolomic profiling, which identified analogous, similar to more lipid differential metabolites, the autophagy pathway and the lysosomal pathway systems, critically involved in cellular homeostasis and lifespan modulation.

3.5.2 Physiological-Transcriptomic Network Interplay Deciphered by Weighted Correlation Network Analysis (WGCNA)

To delineate mechanisms underlying cordycepin-mediated transcriptional regulation of nematode longevity and associated phenotypic adaptations, Weighted Gene Co-expression Network Analysis (WGCNA) was applied to transcriptomic datasets from all treatment groups (Table S9). Phenotype-associated transcriptional networks were resolved via modular clustering of DEGs (FPKM >1), with dynamic hierarchical analysis identifying six co-expression modules (n=4,044 genes; minimum module size=30; Fig. 5A). Eigengene expression patterns exhibited significant correlations with longevity-linked traits, through module-trait interdependencies in a heatmap (Fig. 5B). Strikingly, the Mebrown module (n = 450 genes) exhibited robust positive correlations with lifespan (r = 0.76), body length (r = 0.63), and pharyngeal pumping frequency (r = 0.61; all $P < 0.05$). Similarly, the Meyellow module (n = 309 genes) demonstrated significant positive associations with lifespan (r = 0.69) and body length (r = 0.78; $P < 0.05$). In contrast, the Meturquoise module (n = 1,830 genes) displayed a marked inverse correlation with body length metrics (r = −0.78; $P < 0.05$). Utilizing association criteria k ≥ 100.00; edge weight ≥0.2, we identified 15 high-confidence hub genes within the Mebrown, Meyellow, and Meturquoise co-expression modules (Fig. 5C–E). Transcriptional

profiling revealed opposing regulatory dynamics: the 15 hub genes in both Mebrown and Meyellow modules exhibited pronounced transcriptional upregulation in the C07 group, whereas homologs within the Meturquoise module showed significant downregulation, as validated centrality heatmaps (Fig. 5F–H). Collectively, the 15 high-confidence hub genes identified through WGCNA within the Mebrown, Meyellow, and Meturquoise modules exhibit significant association with modular transcriptional architectures linked to cordycepin-induced lifespan extension in *C. elegans*.

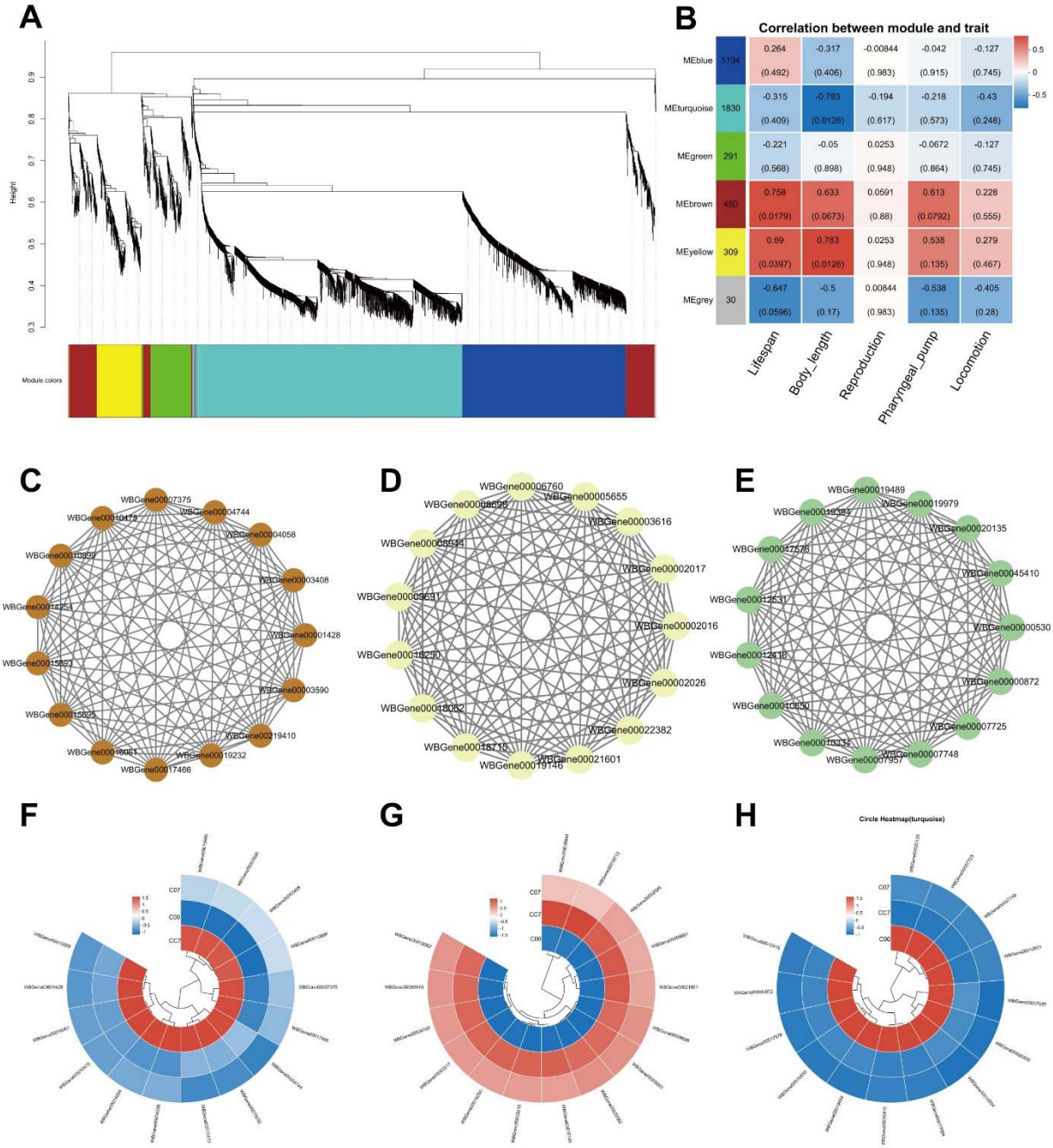

Fig. 5 WGCNA Identifies Longevity-Associated Modules.
(A) Dendrogram of co-expression modules. (B) Module-trait correlations across groups. (C–E) Heatmaps of hub gene expression (MEbrown, MEyellow, MEturquoise). (F–H) Co-expression networks of hub genes with lifespan-related functions. WGCNA, Weighted Gene Co-expression Network Analysis; ME, module eigengene; r, correlation coefficient; C00, control group day 0; C07, control group day 7; CC7, cordycepin treatment day 7.

3.6 Conjoint transcriptome, metabolome, and microbiome analysis

Multi-omics integration was performed to delineate the correlation among microbiome, transcriptome, and metabolome profiles. Sankey diagrams quantified systemic interactions across these omics layers (Fig. 6A). Additionally, correlation heatmaps were employed to delineate the pairwise associations within each omics dataset (Fig. S9). To delineate microbiome-metabolome interdependencies, MIMOSA2 was employed to compute taxon-specific metabolic potential indices, integrating these into a community-wide metabolite potential (CMP) framework (simThreshold = 0.99; signifThreshold = 0.2). In the CC7 vs C07 group, the phylogenetic resolution of microbial contributions identified three high-impact metabolites ($R > 0.8$). Dulcitol and maltotriose demonstrated robust positive associations with *Bacillus* clades (Fig. S10A–D). Meanwhile, glycerol 3-phosphate (G3P), a linchpin metabolite in phospholipid biosynthesis that was significantly increased in cordycepin-treated worms (Fig. 3C), exhibited opposing microbiome associations: its MIMOSA2-derived metabolite potential was strongly positively correlated with *Tumebacillus* abundance (contribution to variance > 1.2) but negatively correlated with *Bacillus* populations (Fig. S10E, F).

Notably, significant correlations emerged between microbial taxa and metabolites, between microbes and host genes, and between host genes and metabolites. These findings imply that microbial communities may modulate nematode longevity by directly or indirectly influencing both metabolite accumulation and gene expression. Moreover, the dynamic alterations in metabolite levels appear to be orchestrated by corresponding genetic regulation. The nine-quadrant diagram further substantiated these observations by revealing robust correlations ($R > 0.75$) between numerous metabolites and gene expression (Fig. 6B; Fig. S11A, B). Finally, the integrated transcriptomic-metabolomic co-enrichment analysis revealed selective pathway perturbations in the CC7 vs C07 comparison, with robust enrichment of ABC transporter, glycerophospholipid metabolism, lysosome, glutathione metabolism, and purine metabolism (Fig. 6C). In the C07 vs C00 contrast, ABC transporter, and autophagy emerged as dominant regulatory hubs (Fig. S11C), while the CC7 vs C00 comparison exhibited enrichment of purine metabolism, glycerophospholipid metabolism, ABC transporter, and glutathione metabolism (Fig. S11D). Integrated network analysis of DEGs and DEMs within statistically enriched biological pathways (Fig. 6D) delineates the functional interconnectivity underlying longevity modulation. Cross-comparative analysis identified fatty acid degradation, FOXO signaling pathway, and glutathione metabolism responses as principal discriminators between experimental groups. These findings suggest a mechanistic convergence whereby cordycepin-induced transcriptional and metabolic reprogramming directly modulates lipid catabolism, stress-responsive signaling and redox buffering systems, functional nodes causally linked to lifespan extension in *C. elegans*.

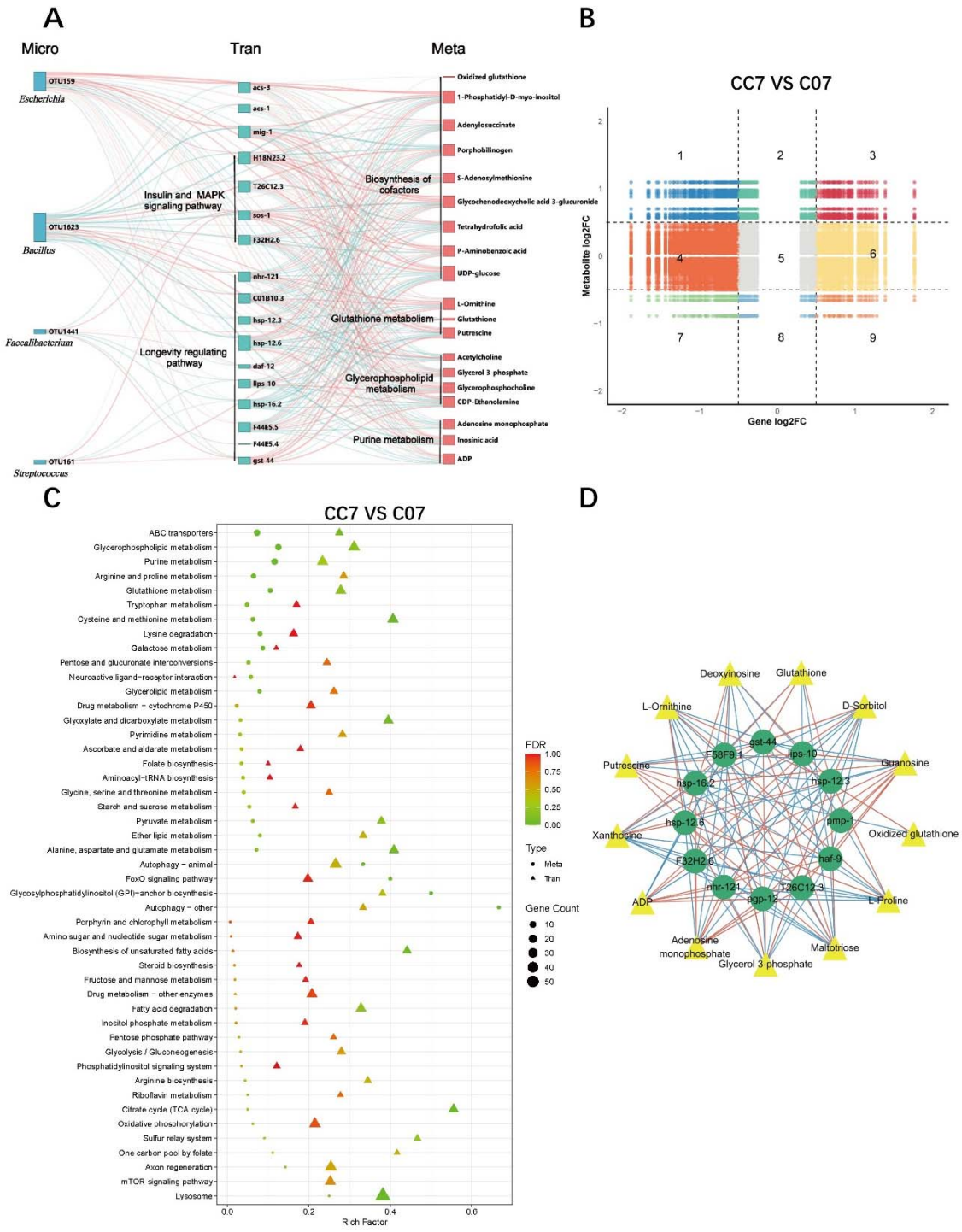

Fig. 6 Multi-Omics Integration Reveals Cordycepin's Systems-Level Effects.
(A) Sankey diagram of microbiota-transcriptome-metabolome interactions. (B) Nine-quadrant analysis of metabolite-gene correlations (CC7 vs C07). (C) KEGG enrichment map of shared pathways (DEGs/DEMs). (D) Integrated network of DEGs-DEMs in enriched processes. OTUs, Operational Taxonomic Units; DEGs, differentially expressed genes; DEMs, differentially expressed metabolites; FC, fold change; KEGG, Kyoto Encyclopedia of Genes and Genomes; FDR, False Discovery Rate; CC7, cordycepin treatment day 7; C07, control group day 7.

3.6.1 Anti-aging target prediction and molecular docking analysis

We employed an integrative network pharmacology workflow to prioritize candidate longevity-associated proteins potentially related to cordycepin action and to guide downstream pathway-level validation. Systematic curation and deduplication of databases yielded 420 putative cordycepin-binding proteins and 409 human longevity-associated proteins (Fig. 7A). Intersection analysis identified 39

overlapping targets (Table S10), which were used to generate a protein-protein interaction (PPI) network via the STRING database (minimum interaction score: 0.700). Subsequent topological analysis using cytoNCA in Cytoscape revealed core network hubs (Fig. 7B), with the insulin-like growth factor receptor (IGF-1R) emerging as a prominent candidate. Notably, DAF-2 is a functional ortholog of mammalian IGF-1R, with conserved structural and mechanistic roles in insulin signaling, which was prioritized for further molecular docking [68, 69]. Molecular docking predicted a favorable interaction between cordycepin and the IGF-1R ligand-binding domain (PDB: 2ZM3; ΔG = −6.67 kcal/mol), with predicted hydrogen-bond contacts at ARG-996, GLN-1073, PRO-1107, and ILE-1205 (Fig. 7C). These docking results provide hypothesis-generating structural insights rather than direct evidence of physical binding. Complementary molecular docking analyses of TGFB1, PTEN, PPARG, and HSP90 further substantiated cordycepin's multi-target engagement (Table S11), reinforcing its may be potential to modulate conserved longevity pathways in *C. elegans*. Although network pharmacology and docking nominate IGF-1R/DAF-2 as a candidate upstream entry point, direct physical binding and biochemical inhibition remain to be established and should be tested in future studies using biophysical and/or biochemical assays.

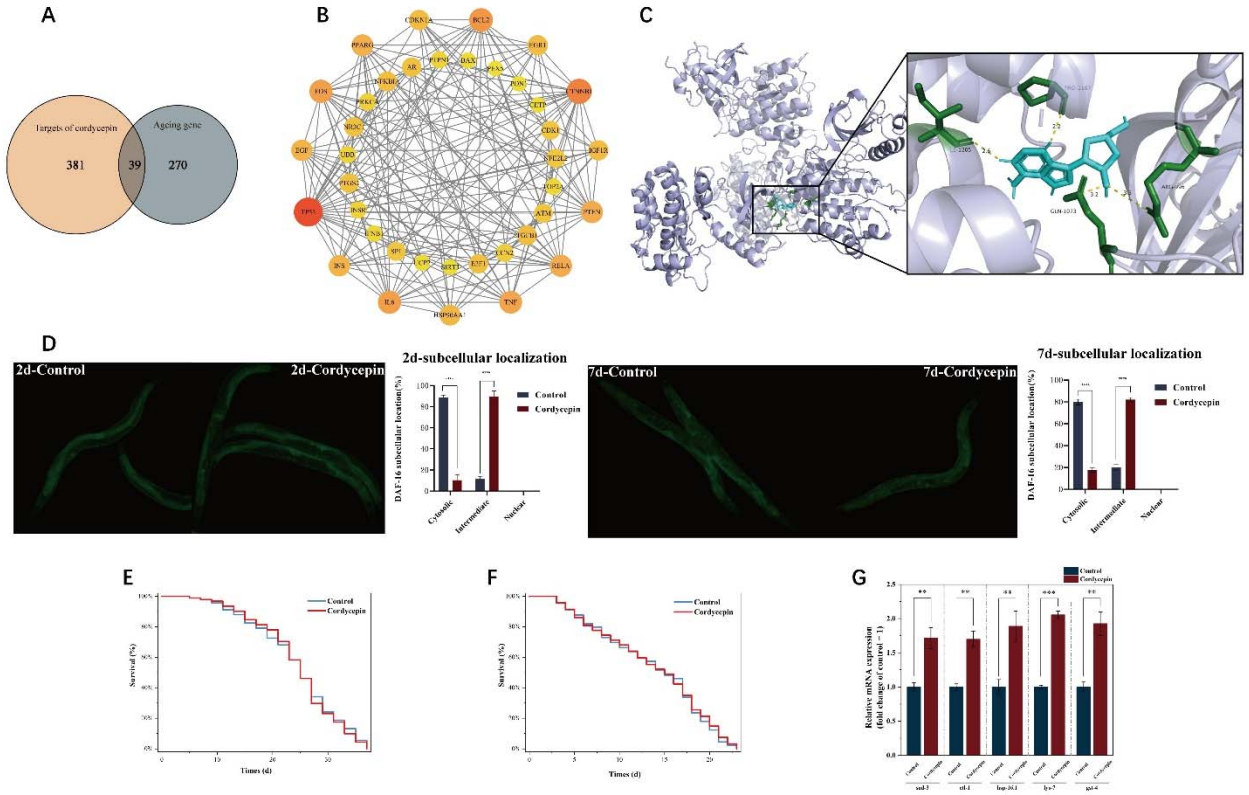

Fig. 7 Cordycepin extends lifespan through IIS/DAF-16 signaling, with IGF-1R/DAF-2 nominated as a candidate upstream node.

(A) Venn diagram of cordycepin targets vs aging-associated proteins (shared nodes highlighted). (B) PPI network of cordycepin targets (node size indicates interaction degree). (C) Docking-based structural prediction of a putative interaction between cordycepin and IGF-1R/DAF-2 (PDB: 2ZM3; predicted hydrogen bonds shown). (D) Representative fluorescence images and quantification of DAF-16::GFP subcellular localization in control and cordycepin-treated worms at adult Day 2 and adult Day 7. Localization was classified as cytosolic, intermediate, or nuclear. (E) Lifespan analysis of *daf-2* (e1370) animals treated with control or cordycepin. (F) Lifespan analysis of *daf-16* (mu86) animals treated with control or cordycepin. (G) RT–qPCR analysis of canonical DAF-16 target genes (*sod-3*, *ctl-1*, *hsp-16.1*, *lys-7*, *gst-4*) in control and cordycepin-treated worms; Data are mean ± SD from 3 biological replicates.**P < 0.01, ***P < 0.001, ****P < 0.0001; IGF-1R, Insulin-like growth factor 1 receptor; PPI, Protein-Protein Interaction; GFP, Green Fluorescent Protein.

3.6.2 Functional validation of IIS/DAF-16 signaling in cordycepin-mediated longevity

To move beyond correlative multi-omics evidence, we performed functional assays to test whether the IIS/DAF-16 axis is required for the cordycepin-induced longevity phenotype. First, we monitored DAF-16 activation using a DAF-16::GFP reporter strain and quantified its subcellular distribution as cytosolic, intermediate, or nuclear. In young adults (Day 2), DAF-16::GFP was predominantly cytosolic in control animals, whereas cordycepin treatment markedly shifted the population toward the intermediate localization state, with essentially no animals exhibiting complete nuclear localization (Fig. 7D). Notably, this activation pattern was maintained during aging: at Day 7, control animals displayed largely cytosolic DAF-16::GFP, while cordycepin-treated animals retained a high proportion of intermediate localization (Fig. 7D). These results indicate that cordycepin promotes a sustained, physiological enrichment of DAF-16 toward the nucleus rather than an acute, fully nuclear translocation. Next, we performed genetic epistasis analyses to determine whether DAF-16 is required for cordycepin-induced lifespan regulation. In the insulin/IGF-1 receptor reduction-of-function mutant *daf-2* (e1370), cordycepin treatment did not further extend lifespan compared with the corresponding control (Fig. 7E), suggesting that cordycepin converges on the IIS/DAF-16 axis when DAF-16 activity is already elevated by reduced IIS. In contrast, in the DAF-16 loss-of-function mutant *daf-16* (mu86), cordycepin failed to extend lifespan and survival curves overlapped between treated and control groups (Fig. 7F), demonstrating that DAF-16 is essential for cordycepin-mediated longevity.

Finally, to link DAF-16 activation to downstream effector programs, we conducted RT–qPCR analysis of representative DAF-16 target genes involved in stress resistance and proteostasis. Cordycepin significantly increased the expression of *sod-3*, *ctl-1*, *hsp-16.1*, *lys-7*, and *gst-4* (Fig. 7G), supporting activation of a DAF-16-dependent protective transcriptional module consistent with the observed organismal outcomes. In contrast, RT–qPCR validation of core AMPK pathway components (*aak-2* and *aakg-1*) did not show reproducible regulation by cordycepin, suggesting that canonical AMPK signaling is not robustly altered under our experimental conditions (Fig. S12). Collectively, the DAF-16::GFP localization, IIS epistasis, and transcriptional profiling results establish a causal chain in which cordycepin activates IIS/DAF-16 signaling, promotes sustained DAF-16 nuclear enrichment, and induces downstream stress-response effectors that contribute to lifespan benefits.

3.6.3 Analysis of Key Pathways Involved in Cordycepin-Induced Lifespan Extension in C. elegans

A convergent multi-omics framework integrating network pharmacology, microbiome, transcriptomic profiling, and metabolomic flux analysis identified the insulin/IGF-1 signaling (IIS)/Forkhead box O (FOXO) signaling pathway as a central regulatory axis underlying cordycepin-mediated lifespan extension in *C. elegans*. Complementary systems-level interrogation revealed coordinated modulation of the TGF-β signaling pathway, delineating a tripartite signaling network governing geroprotective responses (Fig. 8). Mechanistic dissection revealed pronounced IIS transcriptional repression. Cordycepin exposure induced significant *daf-2* suppression (log2FC = −0.74, $P < 0.001$) and downstream effector downregulation (*age-1*, *daf-18*, *pdk-1*, *akt-1/2*; $P < 0.001$), paralleled by PIP3 depletion (−0.86-fold, $P < 0.001$). FOXO activation was evidenced by

fkh-2 (log2FC = +1.21, $P < 0.05$) and *pes-1* upregulation (log2FC = +0.81, $P < 0.05$), indicative of conserved longevity network engagement. In line with the multi-omics signature of elevated GSH, the transcriptome showed a coordinated, isoform-specific modulation of the glutathione metabolism module under cordycepin treatment, encompassing enzymes for GSH biosynthesis and recycling, γ-glutamyl turnover, multiple GSTs, and GSH-dependent peroxidases. This pattern points to a system-level reconfiguration of glutathione-dependent antioxidant capacity rather than a simple, uniform upregulation of individual components. Compensatory TGF-β rewiring manifested as *daf-4*/*daf-3* suppression and *daf-14*/*daf-8* induction, suggesting alterations in SMAD. Metabolomic-transcriptomic integration delineated cordycepin-enhanced stress resilience, marked by glutathione biosynthesis upregulation (*gsto-1*: log2FC = +1.18; GSH: +1.09-fold, $P < 0.05$) and metabolite signatures consistent with altered glycerophospholipid/redox metabolism (*gpdh-2*: log2FC = +0.44; G3P accumulation). Enhanced proteostasis was corroborated by *hsp-70* induction (1.4–2.2 fold; Table S12). However, the present data do not distinguish whether these metabolite changes are causal drivers or downstream consequences of the longevity phenotype.

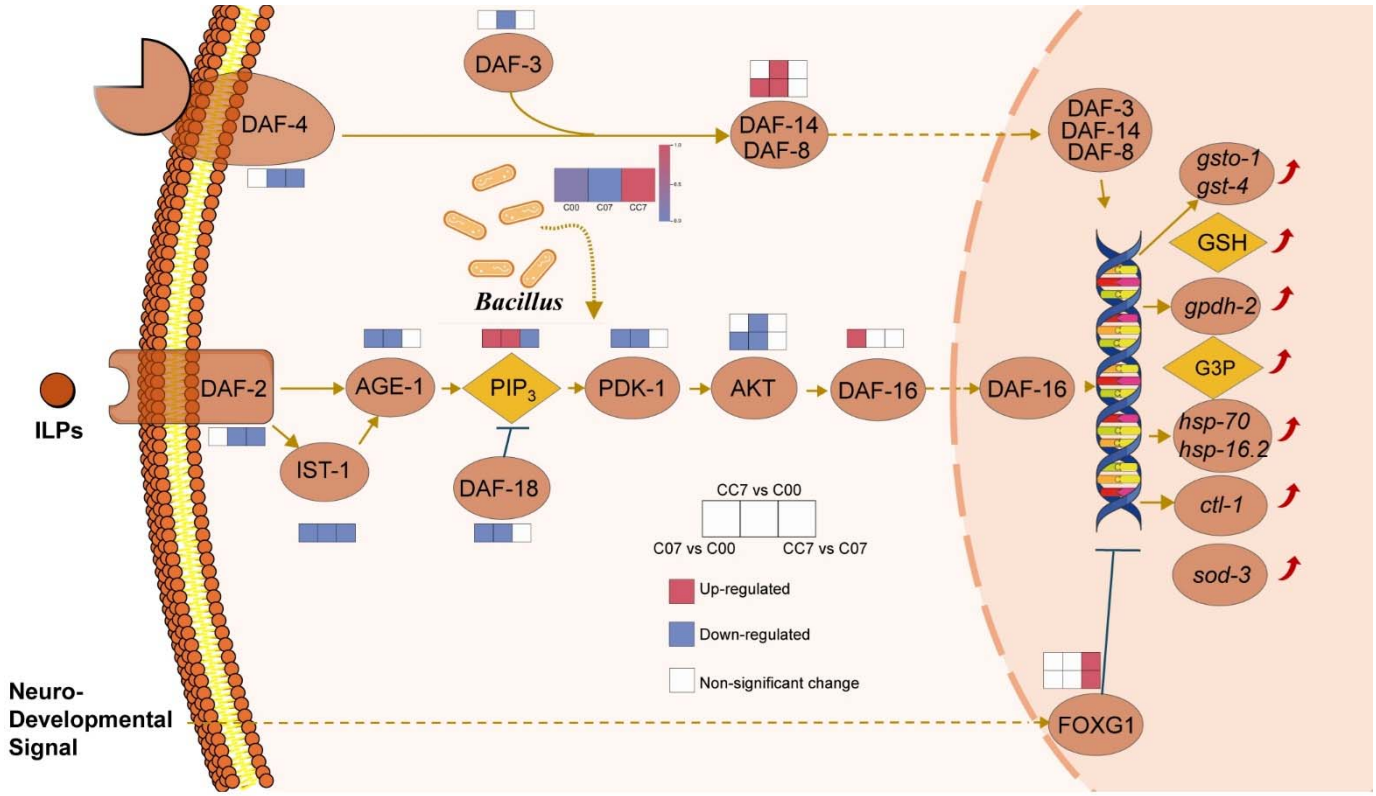

Fig. 8 Mechanistic Framework of Cordycepin-Mediated Longevity in *C. elegans*.
Multi-omics profiling identifies the IIS/FOXO axis as a central regulatory nexus. Cordycepin is proposed to act through IIS-associated upstream nodes (including DAF-2/IGF-1R), promoting DAF-16/FOXO activation to orchestrate stress resilience, autophagy, and metabolic homeostasis. This systemic reprogramming is accompanied by a pro-longevity-associated Bacillus signature and synergistic TGF-β crosstalk. ILPs, Insulin-like peptides; DAF-2, Insulin/IGF-1 receptor; IST-1, Insulin receptor substrate 1; AGE-1, Phosphoinositide 3-kinase; DAF-18, Phosphatase and tensin homolog; PIP3, Phosphatidylinositol (3,4,5)-trisphosphate; PDK-1, 3-phosphoinositide-dependent protein kinase 1; AKT, Protein kinase B; DAF-16, Forkhead box O transcription factor; DAF-4, Type II TGF-β receptor; DAF-8/DAF-14, R-SMADs; DAF-3, Co-SMAD; FOXG1, Forkhead box G1; TGF-β, Transforming growth factor beta; GSH, Glutathione; G3P, Glycerol-3-phosphate; AMP, Adenosine monophosphate.

In conclusion, cordycepin-mediated longevity enhancement in *C. elegans* operates principally through the IIS/FOXO signaling pathway, orchestrating multilayered modulation of downstream effector genes across interconnected metabolic pathways encompassing antioxidant defense, lipid homeostasis, oxidative stress response, and energy flux regulation. Although docking and network pharmacology nominate IGF-1R/DAF-2 as a candidate upstream entry point, direct physical binding and biochemical inhibition remain to be established and should be validated in future studies using SPR/MST/ITC and kinase/competition assays.

4. Discussion

4.1 Response of the nematode microbiome to cordycepin

Aging in animal models is associated with a diminution of microbiome alpha diversity [70-72]. Our findings demonstrate a pronounced reduction in α diversity across aged groups (Table S4). Notably, the CC7 group exhibited significantly elevated α diversity relative to the C07 group, concomitant with a robust enrichment of *Bacillus* spp. in cordycepin-treated specimens. Previous studies have shown that *Bacillus* enhances nematode longevity via biofilm-mediated intestinal colonization, which modulates the DAF-2/DAF-16/HSF-1 signaling axis and suppresses insulin-like signaling (ILS) [73]. Furthermore, *Bacillus amyloliquefaciens* extends *C. elegans* lifespan through activation of JNK and p38 MAPK pathways [74]. Methylglyoxal (MG), a metabolite synthesized by *Bacillus*, governs longevity via the TORC2/SGK-1/DAF-16 cascade [75]. This duality highlights the intricate interplay between microbial pathogenicity and host longevity pathways, wherein insulin/IGF-1 signaling regulates both behavioral avoidance of *Bacillus thuringiensis* and systemic stress resilience [76, 77]. In this study, cordycepin treatment elicited a marked increase in *Bacillus* spp. abundance. Because 16S rRNA V3–V4 sequencing has limited taxonomic resolution, species-level assignments should be interpreted with caution and are not sufficient to claim enrichment of a specific species. This observation aligns with the reported correlation between microbiome shifts and lifespan extension in nematodes. However, based on our current multi-omics data, we define *Bacillus* as a pro-longevity-associated signature taxon rather than the sole determinant. Importantly, our functional data demonstrate that cordycepin-mediated lifespan extension requires DAF-16 activity (Fig. 7F) and converges on the IIS/DAF-16 axis (Fig. 7E). Thus, the microbiome shift may represent an upstream association layer that co-varies with host metabolic remodeling and IIS/DAF-16 activation, linking microbial composition to longevity-relevant host programs at the systems level. Nevertheless, whether microbiome remodeling contributes causally upstream to the DAF-16-dependent benefits of cordycepin warrants further validation. Challenges arise from the inherent complexity of the nematode microbiome and the potential confounding effects of dietary conditions. To address these limitations, future investigations should integrate germ-free nematode models [78], single-bacterium colonization assays [79], and high-resolution metabolomic [80] profiling to disentangle causal relationships between microbial dynamics and lifespan regulation.

4.2 Mechanisms of the Cordycepin-Induced Metabolomic Response in C. elegans

Previous investigations in *C. elegans* have demonstrated that lifespan extension correlates with multimodal metabolic reprogramming [81-83]. Integrated LC-MS-based metabolomic profiling revealed that cordycepin administration elicits a multifaceted metabolic remodeling in *C. elegans*, characterized by the coordinated activation of pathways governing lipid metabolism, purine metabolism, amino acid, and glutathione biosynthesis—adaptations that collectively modulate organismal longevity (Fig. 3; Fig. S6). We posit that these dynamic metabolic shifts, spanning energy metabolism, nucleotide recycling, nitrogen balance, and redox buffering capacity, mechanistically contribute to the observed lifespan extension.

Modulations in lipid metabolic pathways, particularly the enrichment of unsaturated fatty acid species, were demonstrated to correlate with lifespan extension in *C. elegans*. Notably, glycerol-3-phosphate (G3P) emerged as a prominent metabolite associated with the cordycepin-treated state. Beyond its role in buffering free fatty acid flux [84], G3P is the obligate glycerol backbone for de novo glycerophospholipid and triacylglycerol biosynthesis: it is acylated by glycerol-3-phosphate acyltransferases to generate lysophosphatidic acid and phosphatidic acid [85], which are subsequently converted into diacylglycerol and major membrane phospholipids (e.g., phosphatidylcholine and phosphatidylethanolamine) as well as storage triacylglycerols [86, 87]. Therefore, increased G3P availability is consistent with altered membrane phospholipid biogenesis, membrane renewal/repair, and lipid-droplet dynamics, consistent with the lipid remodeling signatures observed in our metabolomic dataset (Fig. 3C). In addition, G3P participates in redox and energy coupling via the glycerol-3-phosphate shuttle, linking cytosolic glycolysis to mitochondrial respiration and contributing to NADH/NAD^+ balance [88]. Together, the elevated G3P levels detected in cordycepin-treated worms (Fig. 3C) are consistent with coordinated lipid–membrane remodeling and cytosolic–mitochondrial redox homeostasis; however, the present data do not determine whether this change is causally upstream of lifespan extension or reflects a downstream feature of the pro-longevity state [85–89]. Modulation of purinergic signaling metabolites underpins lifespan extension via regulation of intracellular energy homeostasis, principally mediated through the AMP: ATP ratio [90]. The marked remodeling of purine metabolic pathways observed following cordycepin administration in this study suggests a plausible mechanistic linkage to this evolutionarily conserved metabolic variation. Amino acid metabolism critically governs *C. elegans* longevity through integrative regulation of cellular bioenergetics, redox equilibrium, signal transduction cascades, and proteostatic mechanisms [91-93]. Metabolomic perturbations within cysteine and methionine metabolism, tryptophan metabolism, and Arginine and proline metabolism demonstrated functional convergence with these lifespan-modulating processes in this investigation. Lifespan extension in nematodes is mechanistically linked to elevated reduced glutathione (GSH) concentrations, which potentiate redox homeostasis [94]. Our multi-omics data indicate that cordycepin promotes thermotolerance and lifespan extension primarily by remodeling a glutathione-centered antioxidant and detoxification network rather than acting through a single enzyme. Cordycepin increases GSH levels, induces *gsto-1* and multiple glutathione S-transferases and GSH-dependent peroxidases, and tends to upregulate GSH biosynthesis and recycling genes, consistent with a coordinated reinforcement of glutathione-based defenses. This glutathione-centered signature parallels

established longevity mechanisms in *C. elegans*, where glutathione reductase, omega-class GSTs, GST-4, and the GSH–GPX-1 axis contribute to stress tolerance and lifespan control [95, 96]. Consistent with this interpretation, targeted RT–qPCR confirmed induction of canonical DAF-16 downstream effectors, including *gst-4* together with stress-resistance and proteostasis genes (sod-3, ctl-1, hsp-16.1, lys-7) (Fig. 7G), supporting engagement of a DAF-16-linked protective module. While our data remains correlative, the convergence of cordycepin-induced glutathione pathway remodeling with these validated mechanisms is consistent with involvement of the glutathione system in the observed longevity phenotype; however, direct tests will be required to determine whether this metabolic signature is causally required for lifespan extension. These findings align with the redox regulatory axis identified in our experimental paradigm. Collectively, our findings demonstrate that cordycepin-mediated lifespan extension in *C. elegans* occurs through coordinated enhancement of lipid-energy metabolic networks and redox stabilization, mechanistically paralleling conserved longevity pathways mediated by FOXO/DAF-16 [97, 98]. The observed membrane restructuring augmentation, amino acid metabolism adjustment, and nutrient signaling modulation suggest functional convergence with evolutionarily conserved mechanisms of metabolic reprogramming and stress resilience. Notably, these metabolite-level changes are mirrored by transcriptome–metabolome association structure in our integrative analyses (Fig. 6B–D), supporting the view that cordycepin engages coordinated molecular modules rather than isolated metabolic events.

4.3 Mechanisms of the Cordycepin-Induced Transcriptional Response in C. elegans

Transcriptomics serves as an indispensable tool for elucidating the molecular mechanisms through which bioactive small molecules modulate longevity in the nematode *C. elegans*. Through comparative analysis of gene expression profiles between treated and untreated groups, we identified pivotal alterations in genes and pathways associated with lifespan extension [99]. For instance, Ginsenoside Rg1 administration induced modulation of the IIS/mTOR signaling axis and influenced genes implicated in neurotransmitter signaling [100, 101]. Prior research has demonstrated that cordycepin extends lifespan via activation of the SKN-1/Nrf2 cascade [102], upregulation of SIRT1 expression [103], sustained telomerase activity, and stimulation of sirtuin family proteins [46]. Consistent with these reports, cordycepin-treated worms in our study exhibited a non-significant trend toward telomere elongation relative to controls ($P > 0.05$). However, although our transcriptomic screen suggested modest changes in selected AMPK-related transcripts, RT–qPCR validation of core AMPK components (*aak-2* and *aakg-1*) did not reveal a reproducible up- or down-regulation under our experimental conditions, suggesting that canonical AMPK signaling is unlikely to be a primary mediator of the observed longevity phenotypes in this model (Fig. S12). AMPK-related genes were therefore treated here as targeted RT–qPCR markers, distinct from the pathway-enrichment results summarized in Fig. 4G. Additionally, transcriptional perturbations were observed in genes governing oxidative stress response, lipid homeostasis, and energy metabolism.

Pathway-centric analysis of longevity regulation in *C. elegans* provides critical insights into the upstream orchestrators of these transcriptional changes. Within the IIS pathway, attenuated signaling facilitates

dephosphorylation and subsequent nuclear translocation of FOXO/DAF-16 [104], activating downstream targets that mediate glucose and fatty acid metabolism, autophagy, antioxidant enzyme production, and DNA repair—processes collectively enhancing cellular resilience and longevity [105-107]. In line with the transcriptomics-centered inference of IIS suppression (Fig. 8), functional imaging of TJ356 (DAF-16::GFP) revealed that cordycepin promotes a sustained, intermediate nuclear enrichment of DAF-16 (predominantly an intermediate localization state) in both younger and older adults (Fig. 7D). This IIS/DAF-16-centered transcriptional shift is consistent with our phenotype-linked network structure (module–trait associations and gene–metabolite correlation patterns), which collectively connect gene programs to lifespan/healthspan outcomes at the systems level.

4.4 Key Pathways Involved in Cordycepin-Induced Lifespan Extension in C. elegans

Multi-omics integration, operating through a systems biology framework, interrogates biological processes holistically to uncover latent molecular mechanisms, synthesize multidimensional biological insights, and enable enhanced predictive modeling capabilities [108]. In this context, MIMOSA2 analysis elucidated putative causal relationships between microbial consortia and metabolic signatures [109]. Targeted metabolomic profiling identified dulcitol, maltotriose, and increased glycerol 3-phosphate as metabolites exhibiting robust microbial covariation. Notably, glycerol 3-phosphate (G3P), a glycerol backbone precursor for de novo glycerophospholipid/triacylglycerol synthesis and a redox-coupling intermediate, has been linked to lifespan-relevant lipid remodeling and metabolic adaptation in *C. elegans* [84-87]. These observations suggest a plausible mechanism whereby the microbiome influences nematode aging through concerted microbial regulation of host metabolite pools, though functional validation via mechanistic dissection of this crosstalk remains imperative. Together, these MIMOSA2-derived associations provide an interaction scaffold linking specific taxa to lifespan-relevant metabolite nodes, which can be further aligned with host transcriptional modules and pathway activity in the subsequent analyses.

Network pharmacology has emerged as a transformative framework for deconvoluting the polypharmacology of bioactive compounds and their disease-modulating mechanisms [110]. For instance, selenium-enriched cordycepin demonstrates efficacy in ameliorating diet-induced obesity, with computational analyses identifying MAPK1, TP53, and TSHR as its primary molecular targets [111]. Intriguingly, our pharmacological network analysis revealed parallels between cordycepin's anti-obesity targets and its longevity-promoting interactome. Specifically, IGF-1R/DAF-2 emerged as a central hub in the predicted longevity-promoting interactome of cordycepin, while DAF-18/PTEN was prioritized as a putative IIS-associated target [112]. These predictions from pharmacological network analysis suggest potential involvement of the IIS pathway in cordycepin's longevity-promoting effects, with IGF-1R/DAF-2 and DAF-18/PTEN highlighted as candidate targets. Independently of the systems-level predictions, we provided functional evidence that cordycepin acts through the IIS/DAF-16 pathway. Cordycepin increased DAF-16::GFP nuclear enrichment without triggering complete nuclear translocation (Fig. 7D). Genetic epistasis further showed that cordycepin did not confer additional lifespan extension in *daf-2* (e1370) mutants

(Fig. 7E), whereas it failed to extend lifespan in the DAF-16 loss-of-function mutant *daf-16* (mu86) (Fig. 7F), demonstrating that DAF-16 is required for the longevity benefit. Consistently, RT–qPCR confirmed induction of representative DAF-16 target genes involved in stress resistance and proteostasis (Fig. 7G). DAF-16::GFP localization revealed a sustained activation pattern: 90-94% of cordycepin-treated exhibited intermediate nuclear enrichment at Day 2, maintained through Day 7 (>80% intermediate), contrasting with acute stress-induced complete nuclear translocation [113]. This physiological activation mode, resembling chronic IIS attenuation via daf-2 mutation rather than emergency stress response [114], likely explains the favorable healthspan profile without growth retardation or reproductive trade-offs [115]. Together, these functional genetic data support the conclusion that cordycepin functionally converges on the IIS/DAF-16 pathway and promotes downstream protective transcriptional programs associated with lifespan extension. Cordycepin also improved survival under acute heat stress (Fig. 1A), indicating enhanced thermotolerance. This phenotype is consistent with reports that multiple longevity-promoting natural products enhance stress resilience via conserved stress-response networks [31–35].

The insulin/IGF-1 signaling (IIS) pathway represents an evolutionarily conserved nexus for longevity regulation [116], wherein its suppression enhances oxidative stress resilience, autophagic flux, and metabolic homeostasis via DAF-16/FOXO activation [96]. Integrating microbiome–metabolite associations (MIMOSA2), transcriptome–metabolome coupling, phenotype-linked co-expression networks, and compound–target predictions with functional validation collectively support the IIS/FOXO axis as a major mediator of cordycepin's geroprotective effects. Cordycepin appears to induce a DAF-16-associated pro-longevity state consistent with partial IIS attenuation, although whether it directly targets an IIS upstream component remains to be determined. Notably, cordycepin exhibited bidirectional modulation of TGF-β signaling, suppressing *daf-3/daf-4* while activating *daf-8/daf-14*, suggesting synergistic crosstalk between TGF-β and IIS cascades in lifespan regulation [117]. Metabolomic profiling revealed diminished AMP pools, indicating remodeling of purine-related metabolites under cordycepin treatment. Although a modest decrease of *aakg-1* transcripts was observed in the RNA-seq dataset, RT–qPCR validation of core AMPK components (*aak-2* and *aakg-1*) did not confirm consistent regulation, arguing against a robust alteration of canonical AMPK signaling in our experimental setting (Fig. S12). Therefore, the AMP decrease observed here is more plausibly interpreted as part of broader purine metabolic remodeling. It is also worth noting that the "0.1 mg/mL" used in C. elegans represents an external plate exposure concentration rather than an administered systemic dose (mg/kg). Because internal exposure in nematodes depends on uptake from the bacterial lawn, absorption, metabolism, and excretion, plate concentration cannot be directly translated into internal exposure metrics (e.g., Cmax/AUC), and a rigorous conversion to a mammalian "equivalent dose" is therefore not appropriate without pharmacokinetic linkage across species. Most purified cordycepin studies used doses ≤50 mg/kg, with many using ≤10 mg/kg, and common administration routes include intraperitoneal and oral/intragastric dosing. Representative mammalian dosing regimens are summarized in Table S13. Moreover, future investigations should focus on three pivotal directions: 1) Establishing definitive causal

links between *Bacillus* spp. enrichment and longevity using Germ-free models or microbiota-depletion strategies; 2) validating direct target engagement of nominated upstream nodes (IGF-1R/DAF-2) using biophysical binding assays (SPR/MST/ITC) and biochemical pathway assays; 3) Mechanistic dissection of pathway crosstalk between IIS/FOXO and TGF-β/SMAD/mTOR networks through Gastrointestinal tract and nervous system genetic manipulations, including direct tests of DAF-16 nuclear transport and RNAi/LOF validation of key DAF-16 effectors; 4) Preclinical evaluation of cordycepin's anti-aging efficacy, including pharmacokinetic and safety profiles in mammalian models. These integrated approaches will advance the understanding of microbiota-host interactions in aging and facilitate therapeutic development.

5. Conclusions

By integrating convergent multi-omics profiling with functional genetics, this study systematically elucidates the molecular mechanisms underlying cordycepin-mediated lifespan extension in *C. elegans*. We establish that cordycepin (0.1-0.5 mg/mL) potentiates longevity by 10-12% under both standard and thermal stress conditions while simultaneously improving multiple healthspan parameters (pharyngeal pumping, locomotion, body length) without detrimental impact on reproductive capacity, underscoring its potential as a favorable healthspan-promoting agent.

Integrative network pharmacology, molecular docking, and functional genetics collectively support the IIS/DAF-16 axis as the principal functionally supported mediator of cordycepin-induced longevity. Genetic epistasis analyses substantiated that DAF-16 is indispensable for the pro-longevity effects of cordycepin, as lifespan extension was abrogated in *daf-16* loss-of-function mutants and showed no additive effect in *daf-2* reduction-of-function animals. This positions cordycepin as a dietary bioactive with dietary-restriction-mimetic–like effects acting through evolutionarily conserved longevity machinery. DAF-16 activation orchestrates coordinated reprogramming across multiple biological layers: (1) Transcriptional level: 3,755 differentially expressed genes enriched in FOXO signaling, autophagy, stress response, and lipid metabolism pathways, with weighted gene co-expression network analysis (WGCNA) identifying 15 hub genes causally linking molecular programs to phenotypic outcomes; (2) Metabolic level: 267 differentially expressed metabolites reflecting glutathione-related antioxidant remodeling and G3P-centered lipid metabolic changes associated with the cordycepin-treated state connecting membrane phospholipid biosynthesis with cytosolic-mitochondrial redox coupling; (3) Microbiome level: selective enrichment of *Bacillus* spp. exhibiting positive correlation with lifespan, consistent with literature reports of *Bacillus*-mediated IIS modulation. Multi-omics integration reveals that these molecular changes converge on shared biological processes (oxidative stress resistance, lipid remodeling, proteostasis), demonstrating holistic systems reprogramming rather than isolated perturbations.

This integrative systems biology framework, progressing from computational target nomination through multi-omics discovery to functional genetic validation, delineates a DAF-16-dependent mechanistic model for cordycepin action and provides a methodological template for dissecting complex natural products. The findings position cordycepin as a promising nutraceutical candidate targeting age-related metabolic

dysregulation through evolutionarily conserved pathways. However, translation to mammalian applications requires systematic pharmacokinetic profiling, long-term safety assessment, and tissue-specific mechanism validation. Future investigations are warranted to: (1) establish microbiome causality through germ-free experiments; (2) define tissue-autonomous vs. non-autonomous DAF-16 contributions; (3) validate direct metabolite-gene regulatory relationships; and (4) conduct preclinical mammalian studies with rigorous toxicological evaluation. These studies will comprehensively define cordycepin's therapeutic window and mechanistic boundaries, advancing rational design of anti-aging interventions addressing the global burden of age-related decline.

Acknowledgment

This work was supported by the Special Fund for Local Science and Technology Development Guided by the Central Government (2024ZYD0252), the Luzhou City Science and Technology Plan Project (2024JYJ104), the Social Livelihood Research and Development Support Project of Chengdu Economic and Technological Development Zone (Longquanyi District) (2024LQRD0045), the Horizontal Science and Technology Project of National Engineering Technology Research Center of Solid-state Brewing (22H1350, PCGS-2022000107), and the Jiangsu Youth Science Foundation (BK20210145).

Declarations

The authors declare that there are no conflicts of interest.

Data availability

Data will be made available on request.

References

[1] E.M. Crimmins, Lifespan and Healthspan: Past, Present, and Promise, Gerontologist. 55 (2015) 901-911. https://doi.org/10.1093/geront/gnv130.

[2] E.M.J.N.A. Crimmins, Recent trends and increasing differences in life expectancy present opportunities for multidisciplinary research on aging, Nature Aging. 1 (2021) 12-13. https://doi.org/10.1038/s43587-020-00016-0.

[3] A. Di Francesco, A.G. Deighan, L. Litichevskiy, et al., Dietary restriction impacts health and lifespan of genetically diverse mice, Nature. 634 (2024) 684-692. https://doi.org/10.1038/s41586-024-08026-3.

[4] M. Izadi, N. Sadri, A. Abdi, et al., Longevity and anti-aging effects of curcumin supplementation, GeroScience. 46 (2024) 2933-2950. https://doi.org/10.1007/s11357-024-01092-5.

[5] S.R. Spindler, P.L. Mote, J.M. Flegal, et al., Influence on longevity of blueberry, cinnamon, green and black tea, pomegranate, sesame, curcumin, morin, pycnogenol, quercetin, and taxifolin fed iso-calorically to long-lived, F1 Hybrid Mice, 16 (2013) 143-151. https://doi.org/10.1089/rej.2012.1386.

[6] Y. Wang, J. Shi, K. Liu, et al., Metabolomics and gene expression levels reveal the positive effects of teaseed oil on lifespan and aging process in *Caenorhabditis elegans*, Food Science and Human Wellness. 12 (2023) 1391-1401. https://doi.org/10.1016/j.fshw.2022.10.032.

[7] A. Goyal, V. Sharma, N. Upadhyay, et al., Flax and flaxseed oil: an ancient medicine & modern functional food, Journal of Food Science and Technology. 51 (2014) 1633-1653. https://doi.org/10.1007/s13197-013-1247-9.

[8] M.S. Hossain, M.A. Kader, K.W. Goh, et al., Herb and Spices in Colorectal Cancer Prevention and Treatment: A Narrative Review, Frontiers in Pharmacology. 13 (2022) 865801. https://doi.org/10.3389/fphar.2022.865801.

[9] Q.-L. Wan, X. Meng, X. Fu, et al., Intermediate metabolites of the pyrimidine metabolism pathway extend the lifespan of *C. elegans* through regulating reproductive signals, Aging. 11 (2019) 3993–4010. https://doi.org/10.18632/aging.102033.

[10] V. Meshram, N.K. Chandrawanshi, Bioactive compounds and pharmacological activities of the genus *Cordyceps*: A review, NewBioWorld A Journal of Alumni Association of Biotechnolog. 4 (2022) 13-19. https://doi.org/10.52228/NBW-JAAB.2022-4-1-4.

[11] T. Peng, J. Guo, X.J.F.i.M. Tong, Advances in biosynthesis and metabolic engineering strategies of cordycepin, Frontiers in Microbiology. 15 (2024) 1386855. https://doi.org/10.3389/fmicb.2024.1386855.

[12] A. Suparmin, T. Kato, H. Dohra, et al., Insight into cordycepin biosynthesis of *Cordyceps militaris*: Comparison between a liquid surface culture and a submerged culture through transcriptomic analysis, PloS one. 12 (2017) e0187052. https://doi.org/10.1371/journal.pone.0187052.

[13] G. Maale, G. Stein, R.J.N. Mans, Effects of cordycepin and cordycepintriphosphate on polyadenylic and ribonucleic acid-synthesising enzymes from eukaryotes, Nature. 255 (1975) 80-82. https://doi.org/10.1038/255080a0.

[14] H.-Y. Pao, B.-M. Huang, M.-Y. Liu, et al. Study of signal transduction pathways activated by cordycepin on steroidogenesis in mouse, Leydig cells.Biology of Reproduction. 78 (2008) 119. https://doi.org/10.1093/biolreprod/78.s1.119a.

[15] L. Tan, X. Song, Y. Ren, et al., Anti-inflammatory effects of cordycepin: A review, Phytotherapy Research. 35 (2021) 1284-1297. https://doi.org/10.1002/ptr.6890.

[16] X. Wang, Y. Li, X. Li, et al., Transcriptome and metabolome profiling unveils the mechanisms of naphthalene acetic acid in promoting cordycepin synthesis in Cordyceps militaris, Frontiers in Nutrition. 10 (2023) 1104446. https://doi.org/10.3389/fnut.2023.1104446.

[17] Y.Y. Wong, A. Moon, R. Duffin, et al., Cordycepin inhibits protein synthesis and cell adhesion through effects on signal transduction, The Journal of Biological Chemistry. 285 (2010) 2610-2621. https://doi.org/10.1074/jbc.M109.071159.

[18] J. Dong, Y. Li, H. Xiao, et al., Cordycepin sensitizes breast cancer cells toward irradiation through elevating ROS production involving Nrf2, Toxicology and Applied Pharmacology. 364 (2019) 12-21. https://doi.org/10.1016/j.taap.2018.12.006.

[19] M.-H. Jeong, M.J. Seo, J.U. Park, et al., Effect of cordycepin purified from *Cordyceps militaris* on Th1 and Th2 cytokines in mouse splenocytes, Journal of Microbiology and Biotechnology. 22 (2012) 1161-1164. https://doi.org/10.4014/jmb.1203.03039.

[20] Q. Jiang, Z. Lou, H. Wang, et al., Antimicrobial effect and proposed action mechanism of cordycepin against *Escherichia coli* and *Bacillus subtilis*, Journal of Microbiology. 57 (2019) 288-297. https://doi.org/10.1007/s12275-019-8113-z.

[21] E. Ryu, M. Son, M. Lee, et al., Cordycepin is a novel chemical suppressor of Epstein-Barr virus replication, Oncoscience. 1 (2014) 866. https://doi.org/10.18632/oncoscience.110.

[22] Y. Wang, Y. Lv, T.S. Liu, et al., Cordycepin suppresses cell proliferation and migration by targeting CLEC2 in human gastric cancer cells via Akt signaling pathway, Life Sciences. 223 (2019) 110-119. https://doi.org/10.1016/j.lfs.2019.03.025.

[23] J. Yang, Y.-z. Li, P.B. Hylemon, et al., Cordycepin inhibits LPS-induced inflammatory responses by modulating NOD-Like Receptor Protein 3 inflammasome activation, Biomedicine & Pharmacotherapy. 95 (2017) 1777-1788. https://doi.org/10.1016/j.biopha.2017.09.103.

[24] X. Zhou, C.U. Meyer, P. Schmidtke, et al., Effect of cordycepin on interleukin-10 production of human peripheral blood mononuclear cells, European journal of pharmacology. 453 (2002) 309-317. https://doi.org/10.1016/s0014-2999(02)02359-2.

[25] R. Di Lorenzo, D. Falanga, L. Ricci, et al., NAD-Driven Sirtuin Activation by Cordyceps sinensis Extract: Exploring the Adaptogenic Potential to Promote Skin Longevity, International Journal of Molecular Sciences. 25 (2024) 4282. https://doi.org/10.3390/ijms25084282.

[26] D.B. Ji, J. Ye, C.L. Li, et al., Antiaging effect of Cordyceps sinensis extract, Phytotherapy Research. 23 (2009) 116-122. https://doi.org/10.1002/ptr.2576.

[27] T. Ramesh, S.-K. Yoo, S.-W. Kim, et al., Cordycepin (3′-deoxyadenosine) attenuates age-related oxidative stress and ameliorates antioxidant capacity in rats, Experimental Gerontology. 47 (2012) 979-987. https://doi.org/10.1016/j.exger.2012.09.003.

[28] H.I. Mack, T. Heimbucher, C.T.J.D.D.T.D.M. Murphy, The nematode *Caenorhabditis elegans* as a model for aging research, Drug Discovery Today: Disease Models. 27 (2018) 3-13. https://doi.org/10.1016/j.ddmod.2018.11.001.

[29] H.A. Tissenbaum, Using *C. elegans* for aging research, Invertebrate reproduction & development, 59 (2015) 59-63. https://doi.org/10.1080/07924259.2014.940470.

[30] S. Zhang, F. Li, T. Zhou, et al., *Caenorhabditis elegans* as a useful model for studying aging mutations, Frontiers in Endocrinology, 11 (2020) 554994. https://doi.org/10.3389/fendo.2020.554994.

[31] P. Li, Z. Wang, S.M. Lam, et al., Rebaudioside A enhances resistance to oxidative stress and extends lifespan and healthspan in *Caenorhabditis elegans*, Antioxidants. 10 (2021) 262. https://doi.org/10.3390/antiox10020262.

[32] E.F. Fang, T.B. Waltz, H. Kassahun, et al., Tomatidine enhances lifespan and healthspan in *C. elegans* through mitophagy induction via the SKN-1/Nrf2 pathway, Scientific Reports. 7 (2017) 46208. https://doi.org/10.1038/srep46208.

[33] R. Xu, A.-P. Li, X. Tan, et al., Patchouli essential oil extends the lifespan and healthspan of Caenorhabditis elegans through JNK-1/DAF-16, Life Sciences. 360 (2025) 123270. https://doi.org/10.1016/j.lfs.2024.123270.

[34] H. Liu, Y. Wang, W. Zhang, et al., Lentinan extends lifespan and increases oxidative stress resistance through DAF-16 and SKN-1 pathways in *Caenorhabditis elegans*, International Journal of Biological Macromolecules. 202 (2022) 286-295. https://doi.org/10.1016/j.ijbiomac.2022.01.071.

[35] K. Lin, J.B. Dorman, A. Rodan, et al., *daf-16*: An HNF-3/forkhead family member that can function to double the life-span of *Caenorhabditis elegans*, Science. 278 (1997) 1319-1322. https://doi.org/10.1126/science.278.5341.1319.

[36] R.K. Junnila, E.O. List, D.E. Berryman, et al., The GH/IGF-1 axis in ageing and longevity, Nature Reviews Endocrinology. 9 (2013) 366-376. https://doi.org/10.1038/nrendo.2013.67.

[37] D.J. Ham, A. Börsch, K. Chojnowska, et al., Distinct and additive effects of calorie restriction and rapamycin in aging skeletal muscle, Nature Communications, 13 (2022) 2025. https://doi.org/10.1038/s41467-022-29714-6.

[38] F. Madeo, D. Carmona-Gutierrez, S.J. Hofer, et al., Caloric restriction mimetics against age-associated disease: targets, mechanisms, and therapeutic potential, Cell Metabolism. 29 (2019) 592-610. https://doi.org/10.1016/j.cmet.2019.01.018.

[39] B. Lant, K.B. Storey, An overview of stress response and hypometabolic strategies in Caenorhabditis elegans: conserved and contrasting signals with the mammalian system, International Journal of Biological Sciences. 6 (2010) 9. https://doi.org/10.7150/ijbs.6.9.

[40] B. Leiers, A. Kampkötter, C.G. Grevelding, et al., A stress-responsive glutathione S-transferase confers resistance to oxidative stress in *Caenorhabditis elegans*, Free Radical Biology and Medicine. 34 (2003) 1405-1415. https://doi.org/10.1016/s0891-5849（03）00102-3.

[41] B. Lant, K.B. Storey, An overview of stress response and hypometabolic strategies in *Caenorhabditis elegans*: conserved and contrasting signals with the mammalian system, International Journal of Biological Sciences. 6 (2010) 9-50. https://doi.org/10.7150/ijbs.6.9.

[42] F. Macedo, T. Romanatto, C. Gomes de Assis, et al., Lifespan-extending interventions enhance lipid-supported mitochondrial respiration in *Caenorhabditis elegans*, The FASEB Journal. 34 (2020) 9972-9981. https://doi.org/10.1096/fj.201901880R.

[43] N. Sun, R.J. Youle, T. Finkel, The mitochondrial basis of aging, Molecular Cell. 61 (2016) 654-666. https://doi.org/10.1016/j.molcel.2016.01.028.

[44] S. Brenner,9The genetics of *Caenorhabditis elegans*, Genetics. 77 (1974) 71-94. https://doi.org/10.1093/genetics/77.1.71.

[45] T. Stiernagle, Maintenance of *C. elegans*, WormBook: The online review of *C. elegans* biology [Internet]. (2006), https://doi.org/10.1895/wormbook.1.101.1.

[46] X. Wang, X. Wang, L. Li, et al., Lifespan extension in *Caenorhabditis elegans* by DMSO is dependent on *sir-2.1* and *daf-16*, Biochemical and Biophysical Research Communications. 400 (2010) 613-618. https://doi.org/10.1016/j.bbrc.2010.08.113.

[47] E. Dehghan, Y. Zhang, B. Saremi, et al., Hydralazine induces stress resistance and extends *C. elegans* lifespan by activating the NRF2/SKN-1 signalling pathway, Nature Communications. 8 (2017) 2223. https://doi.org/10.1038/s41467-017-02394-3.

[48] C.J. Gaffney, A. Pollard, T.F. Barratt, et al., Greater loss of mitochondrial function with ageing is associated with earlier onset of sarcopenia in *C. elegans*, Aging. 10 (2018) 3382. https://doi.org/10.18632/aging.101654.

[49] H.S. Choi, A. Bhat, M.B. Howington, et al., FMO rewires metabolism to promote longevity through tryptophan and one carbon metabolism in C. elegans, Nature Communications. 14 (2023) 562. https://doi.org/10.1038/s41467-023-36181-0.

[50] J.P. Ke, J.Y. Yu, B. Gao, et al., Two new catechins from Zijuan green tea enhance the fitness and lifespan of Caenorhabditis elegans via insulin-like signaling pathways, Food & Function. 13 (2022) 9299-9310. https://doi.org/10.1039/d2fo01795d.

[51] D. Raizen, B.-m. Song, N. Trojanowski, et al., Methods for measuring pharyngeal behaviors, WormBook: The Online Review of *C. elegans* Biology [Internet]. (2018), https://doi.org/10.1895/wormbook.1.154.1.

[52] H. Wang, P. Webster, L. Chen, et al., Cell-autonomous and non-autonomous roles of *daf-16* in muscle function and mitochondrial capacity in aging *C. elegans*, Aging. 11 (2019) 2295. https://doi.org/10.18632/aging.101914.

[53] T. Magoč, S.L. Salzberg, FLASH: fast length adjustment of short reads to improve genome assemblies, Bioinformatics. 27 (2011) 2957-2963. https://doi.org/10.1093/bioinformatics/btr507.

[54] J.G. Caporaso, J. Kuczynski, J. Stombaugh, et al., QIIME allows analysis of high-throughput community sequencing data, Nature Methods. 7 (2010) 335-336. https://doi.org/10.1038/nmeth.f.303.

[55] R.C. Edgar, UPARSE: highly accurate OTU sequences from microbial amplicon reads, Nature Methods. 10 (2013) 996-998. https://doi.org/10.1016/j.taap.2018.12.006.

[56] B.L. Maidak, J.R. Cole, T.G. Lilburn, et al., The RDP (ribosomal database project) continues, Nucleic Acids Research. 28 (2000) 173-174. https://doi.org/10.1093/nar/28.1.173.

[57] J.E. Walker, J.C. Oliver, A.M. Stewart, et al., Measuring Up: A Comparison of TapeStation 4200 and Bioanalyzer 2100 as Measurement Tools for RNA Quality in Postmortem Human Brain Samples, International Journal of Molecular Sciences. 24 (2023) https://doi.org/10.3390/ijms241813795.

[58] M. Kanehisa, M. Furumichi, M. Tanabe, et al., KEGG: new perspectives on genomes, pathways, diseases and drugs, Nucleic Acids Research. 45 (2017) D353-D361. https://doi.org/10.1093/nar/gkw1092.

[59] Z. Jiang, W. Su, M. Yang, et al., Integrated multi-omics reveals the *Bacillus amyloliquefaciens* BA40 against *Clostridium* perfringens infection in weaned piglets, Journal of Advanced Research. 77 (2025): 75-90. https://doi:10.1016/j.jare.2025.01.033.

[60] J. Yao, Y. Jiang, P. Zhang, et al., Genetic and pharmacological targeting of HINT2 promotes OXPHOS to alleviate inflammatory responses and cell necrosis in acute pancreatitis, Pharmacological Research. 212 (2025) 107620. https://doi.org/10.1016/j.phrs.2025.107620.

[61] D.E. Cook, S. Zdraljevic, R.E. Tanny, et al., The genetic basis of natural variation in *Caenorhabditis elegans* telomere length, Genetics. 204 (2016) 371-383. https://doi.org/10.1534/genetics.116.191148.

[62] Z. Qi, H. Ji, M. Le, et al., Sulforaphane promotes *C. elegans* longevity and healthspan via DAF-16/DAF-2 insulin/IGF-1 signaling, Aging . 13 (2021) 1649-1670. https://doi.org/10.18632/aging.202512.

[63] B. Viollet, M. Foretz, Animal Models to Study AMPK, Experientia supplementum (2012). 107 (2016) 441-469. https://doi.org/10.1007/978-3-319-43589-3_18.

[64] L. Fontana, L. Partridge, V.D. Longo, Extending healthy life span—from yeast to humans, Science. 328 (2010) 321-326. https://doi.org/10.1126/science.1172539.

[65] J.-F. Lemaître, V. Berger, C. Bonenfant, et al., Early-late life trade-offs and the evolution of ageing in the wild, Proceedings of the Royal Society B: Biological Sciences. 282 (2015) 20150209. https://doi.org/10.1098/rspb.2015.0209.

[66] S. Li, J.M. Vazquez, P.H. Sudmant, The evolution of aging and lifespan, Trends in Genetics. 39 (2023) 830-843. https://doi.org/ 10.1016/j.tig.2023.08.005.

[67] N.M. Templeman, C.T. Murphy, Regulation of reproduction and longevity by nutrient-sensing pathways, Journal of Cell Biology. 217 (2018) 93-106. https://doi.org/10.1083/jcb.201707168.

[68] K.D. Kimura, H.A. Tissenbaum, Y. Liu, et al., *daf-2*, an insulin receptor-like gene that regulates longevity and diapause in *Caenorhabditis elegans*, Science. 277 (1997) 942-946. https://doi.org/10.1126/science.277.5328.942.

[69] S.B. Pierce, M. Costa, R. Wisotzkey, et al., Regulation of DAF-2 receptor signaling by human insulin and *ins-1*, a member of the unusually large and diverse *C. elegans* insulin gene family, Genes & development. 15 (2001) 672-686. https://doi.org/10.1101/gad.867301.

[70] B. Sadoughi, D. Schneider, R. Daniel, et al., Aging gut microbiota of wild macaques are equally diverse, less stable, but progressively personalized, Microbiome. 10 (2022) 95. https://doi.org/10.1186/s40168-022-01283-2.

[71] M.S. Spychala, V.R. Venna, M. Jandzinski, et al., Age-related changes in the gut microbiota influence systemic inflammation and stroke outcome, Annals of Neurology. 84 (2018) 23-36. https://doi.org/10.1002/ana.25250.

[72] T. Wilmanski, C. Diener, N. Rappaport, et al., Gut microbiome pattern reflects healthy ageing and predicts survival in humans, Nature Metabolism. 3 (2021) 274-286. https://doi.org/10.1038/s42255-021-00348-0.

[73] V. Donato, F.R. Ayala, S. Cogliati, et al., *Bacillus subtilis* biofilm extends *Caenorhabditis elegans* longevity through downregulation of the insulin-like signalling pathway, Nature Communications. 8 (2017) 14332. https://doi.org/10.1038/ncomms14332.

[74] M.R. Park, S. Oh, S.J. Son, et al., *Bacillus licheniformis* isolated from traditional Korean food resources enhances the longevity of *Caenorhabditis elegans* through serotonin signaling, Journal of Agricultural and Food Chemistry. 63 (2015) 10227-10233. https://doi.org/10.1021/acs.jafc.5b03730.

[75] M.-G. Shin, J.-W. Lee, J.-S. Han, et al., Bacteria-derived metabolite, methylglyoxal, modulates the longevity of *C. elegans* through TORC2/SGK-1/DAF-16 signaling, Proceedings of the National Academy of Sciences. 117 (2020) 17142-17150. https://doi.org/10.1073/pnas.1915719117.

[76] M. Hasshoff, C. Höhnisch, D. Tonn, et al., The role of *Caenorhabditis elegans* insulin-like signaling in the behavioral avoidance of pathogenic *Bacillus thuringiensis*, The FASEB Journal. 21 (2007) 1801-1812. https://doi.org/10.1096/fj.06-6551com.

[77] B. Wang, H. Wang, J. Xiong, et al., A proteomic analysis provides novel insights into the stress responses of *Caenorhabditis elegans* towards nematicidal Cry6A Toxin from *Bacillus thuringiensis*, Scientific Reports. 7 (2017) 14170. https://doi.org/10.1038/s41598-017-14428-3.

[78] F. Aghighi, M. Salami, What we need to know about the germ-free animal models, AIMS Microbiology. 10 (2024) 107-147. https://doi.org/10.3934/microbiol.2024007.

[79] S.M. Lee, G.P. Donaldson, Z. Mikulski, et al., Bacterial colonization factors control specificity and stability of the gut microbiota, Nature. 501 (2013) 426-429. https://doi.org/10.1038/nature12447.

[80] M.M. Niedzwiecki, D.I. Walker, J.C. Howell, et al., High-resolution metabolomic profiling of Alzheimer's disease in plasma, Annals of Clinical and Translational Neurology. 7 (2020) 36-45. https://doi.org/10.1002/acn3.50956.

[81] N. Copes, C. Edwards, D. Chaput, et al., Metabolome and proteome changes with aging in *Caenorhabditis elegans*, Experimental Gerontology. 72 (2015) 67-84. https://doi.org/10.1016/j.exger.2015.09.013.

[82] S. Fuchs, J.G. Bundy, S.K. Davies, et al., A metabolic signature of long life in *Caenorhabditis elegans*, BMC biology. 8 (2010) 1-12. https://doi.org/10.1186/1741-7007-8-14.

[83] G.A. Lemieux, K. Ashrafi, Investigating connections between metabolism, longevity, and behavior in *Caenorhabditis elegans*, Trends in Endocrinology & Metabolism. 27 (2016) 586-596. https://doi.org/10.1016/j.tem.2016.05.004.

[84] K. Tighanimine, J.A. Nabuco Leva Ferreira Freitas, I. Nemazanyy, et al., A homoeostatic switch causing glycerol-3-phosphate and phosphoethanolamine accumulation triggers senescence by rewiring lipid metabolism, Nature Metabolism. 6 (2024) 323-342. https://doi.org/10.1038/s42255-023-00972-y.

[85] V.T. Samuel, G.I. Shulman, The pathogenesis of insulin resistance: integrating signaling pathways and substrate flux, The Journal of Clinical Investigation. 126 (2016) 12-22. https://doi.org/10.1172/JCI77812.

[86] P. Schönfeld, L. Wojtczak, Short-and medium-chain fatty acids in energy metabolism: the cellular perspective, Journal of Lipid Research. 57 (2016) 943-954. https://doi.org/10.1194/jlr.R067629.

[87] K. Takeuchi, K. Reue, Biochemistry, physiology, and genetics of GPAT, AGPAT, and lipin enzymes in triglyceride synthesis, American Journal of Physiology-Endocrinology and Metabolism. 296 (2009) E1195-E1209. https://doi.org/10.1152/ajpendo.90958.2008.

[88] T. Mráček, Z. Drahota, J. Houštěk, The function and the role of the mitochondrial glycerol-3-phosphate dehydrogenase in mammalian tissues, Biochimica et Biophysica Acta (BBA)-Bioenergetics. 1827 (2013) 401-410. https://doi.org/10.1016/j.bbabio.2012.11.014.

[89] M. Agassandian, R.K. Mallampalli, Surfactant phospholipid metabolism, Biochimica et Biophysica Acta (BBA)-Molecular and Cell Biology of Lipids. 1831 (2013) 612-625. https://doi.org/10.1016/j.bbalip.2012.09.010.

[90] L.E.B. Savio, R. Leite-Aguiar, V.S. Alves, et al., Purinergic signaling in the modulation of redox biology, Redox biology. 47 (2021) 102137. https://doi.org/10.1016/j.redox.2021.102137.

[91] X. Feng, X. Wang, L. Zhou, et al., The impact of glucose on mitochondria and life span is determined by the integrity of proline catabolism in *Caenorhabditis elegans*, Journal of Biological Chemistry. 299 (2023), https://doi.org/10.1016/j.jbc.2023.102881.

[92] H.A. Miller, S. Huang, E.S. Dean, et al., Serotonin and dopamine modulate aging in response to food odor and availability, Nature Communications. 13 (2022) 3271. https://doi.org/10.1038/s41467-022-30869-5.

[93] A.A. Parkhitko, P. Jouandin, S.E. Mohr, et al., Methionine metabolism and methyltransferases in the regulation of aging and lifespan extension across species, Aging Cell. 18 (2019) e13034. https://doi.org/10.1111/acel.13034.

[94] V.I. Lushchak, Glutathione homeostasis and functions: potential targets for medical interventions, Journal of Amino Acids. 2012 (2012) 736837. https://doi.org/10.1155/2012/736837.

[95] C.S. Kaiser, M. Lubisch, E. Schroder, et al., Unraveling the functional dynamics of Caenorhabditis elegans stress-responsive omega class GST-44, The FEBS journal. 292 (2025) 4675-4693. https://doi.org/10.1111/febs.70088.

[96] W. Qian, J. Lu, T. Wang, et al., Isobavachalcone confers protection against Cryptococcus neoformans-induced ferroptosis in Caenorhabditis elegans via lifespan extension and GSH-GPX-1 axis modulation, Journal of Hazardous Materials. 492 (2025) 137969. https://doi.org/10.1016/j.jhazmat.2025.137969.

[97] A.W. Gao, R.L. Smith, M. Van Weeghel, et al., Identification of key pathways and metabolic fingerprints of longevity in *C. elegans*, Experimental Gerontology. 113 (2018) 128-140. https://doi.org/10.1016/j.exger.2018.10.003.

[98] X. Sun, W.-D. Chen, Y.-D. Wang, DAF-16/FOXO transcription factor in aging and longevity, Frontiers in Pharmacology. 8 (2017) 548. https://doi.org/10.3389/fphar.2017.00548.

[99] A.E. Tarkhov, R. Alla, S. Ayyadevara, et al., A universal transcriptomic signature of age reveals the temporal scaling of *Caenorhabditis elegans* aging trajectories, Scientific Reports. 9 (2019) 7368. https://doi.org/10.1038/s41598-019-43075-z.

[100] H. Wang, S. Zhang, L. Zhai, et al., Ginsenoside extract from ginseng extends lifespan and health span in *Caenorhabditis elegans*, Food & Function. 12 (2021) 6793-6808. https://doi.org/10.1039/d1fo00576f.

[101] X. Yu, H. Li, D. Lin, et al., Ginsenoside prolongs the lifespan of *C. elegans* via lipid metabolism and activating the stress response signaling pathway, International Journal of Molecular Sciences. 22 (2021) 9668. https://doi.org/10.3390/ijms22189668.

[102] Z. Wang, Z. Chen, Z. Jiang, et al., Cordycepin prevents radiation ulcer by inhibiting cell senescence via NRF2 and AMPK in rodents, Nature Communications. 10 (2019) 2538. https://doi.org/10.1038/s41467-019-10386-8.

[103] P. Chueaphromsri, P. Kunhorm, R. Phonchai, et al., Cordycepin enhances SIRT1 expression and maintains stemness of human mesenchymal stem cells, in vivo. 37 (2023) 596-610. https://doi.org/10.21873/invivo.13118.

[104] A. Mukhopadhyay, S.W. Oh, H.A. Tissenbaum, Worming pathways to and from DAF-16/FOXO, Experimental Gerontology. 41 (2006) 928-934. https://doi.org/10.1016/j.exger.2006.05.020.

[105] S.W. Oh, A. Mukhopadhyay, N. Svrzikapa, et al., JNK regulates lifespan in *Caenorhabditis elegans* by modulating nuclear translocation of forkhead transcription factor/DAF-16, Proceedings of the National Academy of Sciences. 102 (2005) 4494-4499. https://doi.org/10.1073/pnas.0500749102.

[106] A. Zečić, B.P. Braeckman, DAF-16/FoxO in *Caenorhabditis elegans* and its role in metabolic remodeling, Cells. 9 (2020) 109. https://doi.org/10.3390/cells9010109.

[107] L. Zhang, B. Gu, Y. Wang, Clove essential oil confers antioxidant activity and lifespan extension in *C. elegans* via the DAF-16/FOXO transcription factor, Comparative Biochemistry and Physiology Part C: Toxicology & Pharmacology. 242 (2021) 108938. https://doi.org/10.1016/j.cbpc.2020.108938.

[108] J. Lan, J.A. Rollins, X. Zang, et al., Translational regulation of non-autonomous mitochondrial stress response promotes longevity, Cell Reports. 28 (2019) 1050-1062. https://doi.org/10.1016/j.celrep.2019.06.078.

[109] C. Noecker, A. Eng, E. Muller, et al., MIMOSA2: a metabolic network-based tool for inferring mechanism-supported relationships in microbiome-metabolome data, Bioinformatics. 38 (2022) 1615-1623. https://doi.org/10.1093/bioinformatics/btac003.

[110] A.L. Hopkins, Network pharmacology, Nature Biotechnology. 25 (2007) 1110-1111. https://doi.org/10.1038/nbt1007-1110.

[111] Z. Zhu, A. Huang, M. Chen, et al., Impacts of selenium enrichment on nutritive value and obesity prevention of Cordyceps militaris: A nutritional, secondary metabolite, and network pharmacological analysis, Food Chemistry: X. 19 (2023) 100788. https://doi.org/10.1016/j.fochx.2023.100788.

[112] S. Ogg, G. Ruvkun, The *C. elegans* PTEN homolog, DAF-18, acts in the insulin receptor-like metabolic signaling pathway, Molecular Cell. 2 (1998) 887-893. https://doi.org/10.1016/s1097-2765(00)80303-2.

[113] K. Warnhoff, J.T. Murphy, S. Kumar, et al., The DAF-16 FOXO transcription factor regulates natc-1 to modulate stress resistance in *Caenorhabditis elegans*, linking insulin/IGF-1 signaling to protein N-terminal acetylation, PLoS Genetics. 10 (2014) e1004703.https://doi.org/10.1371/journal.pgen.1004703.

[114] S.T. Li, H.Q. Zhao, P. Zhang, et al., DAF-16 stabilizes the aging transcriptome and is activated in mid-aged Caenorhabditis elegans to cope with internal stress, Aging Cell. 18 (2019) e12896. https://doi.org/10.1111/acel.12896.

[115] A. Bartke, L.Y. Sun, V. Longo, Somatotropic signaling: trade-offs between growth, reproductive development, and longevity, Physiological reviews. 93 (2013) 571-598. https://doi.org/10.1152/physrev.00006.2012.

[116] O. Altintas, S. Park, S.-J.V. Lee, The role of insulin/IGF-1 signaling in the longevity of model invertebrates, *C. elegans* and *D. melanogaster*, BMB Reports. 49 (2016) 81. https://doi.org/10.5483/bmbrep.2016.49.2.261.

[117] W.M. Shaw, S. Luo, J. Landis, et al., The *C. elegans* TGF-β dauer pathway regulates longevity via insulin signaling, Current Biology. 17 (2007) 1635-1645. https://doi.org/10.1016/j.cub.2007.08.058.